# Stony Brook University

**Macrocyclic Host-Guest Framework for Polymerization of Diiodobutadiyne**

A Thesis Presented

by

**Xianzhi Liu**

to

The Graduate School

in Partial Fulfillment of the

Requirements

for the Degree of

**Master of Science**

in

**Chemistry**

Stony Brook University

**August 2013**

**Stony Brook University**

The Graduate School

**Xianzhi Liu**

We, the thesis committee for the above candidate for the

Master of Science degree, hereby recommend

acceptance of this thesis.

**Dr. Nancy S. Goroff – Thesis Advisor**
**Associate Professor, Department of Chemistry**

**Dr. Joseph W. Lauher - Chairperson of Defense**
**Professor, Department of Chemistry**

**Dr. Jonathan G. Rudick - Third Member of Defense**
**Assistant Professor, Department of Chemistry**

This thesis is accepted by the Graduate School

Charles Taber
Interim Dean of the Graduate School

Abstract of the Thesis

**Macrocyclic host-guest framework for polymerization of diiodobutadiyne**

by

**Xianzhi Liu**

**Master of Science**

in

**Chemistry**

Stony Brook University

**2013**

Conjugated organic polymers have optical and electronic properties that make them candidates for applications in organic field effect transistors (OFETs) and light emitting materials. Polydiacetylenes (PDAs) are an important branch of conjugated polymers with alternating poly(ene-yne) structure. The all-carbon polymer without any side groups is carbyne, which has only alternating single and triple carbon-carbon bonds. Carbyne provides a good opportunity to investigate the inherent properties of conjugated polymers. Polydiiododiacetylene (PIDA), a simple PDA with only iodine atom substituents, can be successfully obtained by the topochemical polymerization of the monomer diiodobutadiyne. This polymerization is achieved through the use of bis(nitrile) or bis(pyridyl) hosts, which hold the monomer in the correct orientation for polymerization by a halogen bond between the Lewis-basic nitrogen and the Lewis-acidic iodine. With the goal of forming carbyne, PIDA has been partially dehalogenated by Lewis bases such as pyrollidine, however, inter-and intramolecular aggregation prevented full dehalogenation.

In this project, an innovative macrocyclic host-guest framework was designed and evaluated for the preparation of PIDA. The macrocyclic host has the function of keeping individual PIDA strands separate and elongated so that Lewis bases can access all the iodine. The macrocyclic host should be able to self-assemble into a tubular framework with enough inner space to accommodate the monomer, diiodobutadiyne. This host should also possess a nitrogen group that can weakly interact with the monomer to hold it in place. Finally, the host should have solubility commensurate with the monomer, since co-crystallization is carried out by slow evaporation. Several possible designs were proposed and computational modeling was performed to analyze the relation between conformation and ring size, as well as whether or not there is a need for a rigidity-increasing segment and a solubility-increasing segment. Based on the evaluation, the target molecule was selected for synthesis. Several steps have been optimized in the synthesis of the macrocyclic host, including hydroxylation and PEG-tosylation of 2,6-dibromopyridine, followed by a Sonogashira coupling with an alkyne-functionalized phthalimide group. Hydrazinolysis was attempted on a model compound and the host precursor to convert the phthalimide group into the amine. Several other detour routes were considered, including Boc protection on the amine before Sonogashira coupling.

**Dedication Page**

**This thesis is dedicated to my dear parents:**

***Chengwei LIU and Xin LU***

## Table of Contents

**List of Figures** ..... **viii**
**List of Schemes** ..... **ix**
**List of Tables** ..... **x**
**Acknowledgment** ..... **xi**

**Chapter 1. Introduction** ..... 3
1.1 Conjugated Polymer and Its Important Branch: Polydiacetylenes ..... 3
1.2 Host-Guest Strategy and Topochemical Polymerization ..... 6
1.3 Dehalogenation of PIDA and the Remained Challenges ..... 8
1.3.1 Host Self-Assembling ..... 8
1.3.2 Host Guest Interactions ..... 10
1.3.3 Application of Halogen Bond, Host-Guest Strategy and Topochemical Polymerization for the Preparation of Polydiiododiacetylene ..... 11
1.3.4 Dehalogenation of PIDA ..... 14

**Chapter 2. Discussion and Results** ..... 16
2.1 Host Design ..... 16
2.1.1 Design for Self-Assembling Function ..... 18
2.1.2 Design for Host-Guest Cooperation ..... 18
2.1.3 Adjustment for Solubility and Ring Flexibility ..... 19
2.1.4 Geometry Calculation ..... 20

2.2 Computational Simulation of Conformation ..... 22
2.2.1 General Introduction of Computational Modeling and Spartan ..... 22
2.2.2 Basic Level Molecular Mechanics Calculation ..... 23
2.2.3 Equilibrium Conformers Using MMFF ..... 25
2.2.4 Higher Level Quantum Chemical Calculation ..... 27

2.3 Synthesis ..... 29
2.3.1 Functionalization on para Site of 2,6-Dibromopyridine ..... 31
2.3.2 Functionalization on 4-Pentyne-1-ol and the Coupling with Pyridyl ..... 33
2.3.3 The Preparation of 2,6-Di-2-(pent-4-ynyl)-1-amino-4-[2-(2-hydroxyethyloxy) ethyloxy]pyridine ..... 35
2.3.4 Model Test for the Reaction of Pentynyl-amine **10** and Ethyl Oxalyl Chloride ..... 40
2.3.5 Model Test for the Crude Product of Pentynyl-amine **10** ..... 40
2.3.6 Model Test for Crude Di-amine-pyridine **9** ..... 41
2.3.7 Alternative Route ..... 42
2.3.8 Future Plan ..... 43
2.4 Conclusion ..... 45

**Chapter 3. Experimental** ..... 45
3.1 Conformation Searching Algorithms ..... 47
3.2 Method for Molecular Mechanics and Quantum Chemical Calculation ..... 47
3.3 Synthesis ..... 48

**Reference** ..... 55

## List of Figures

**Figure 1.1** Representative conjugated polymers ..... 4
**Figure 1.2** Polyyne and carbyne..... 4
**Figure 1.3** Dehydrohalogenation of polymers ..... 5
**Figure 1.4** Geometry for 1,4 polymerization of diacetylene ..... 7
**Figure 1.5** Spatial movement illustration of topochemical polymerization: a monomer single crystal transforms into the polymer single crystal. ..... 7
**Figure 1.6** Host that self-assembled into hydrogen bonding networks ..... 9
**Figure 1.7** Diverse acid-base intermolecular interaction of pyridines..... 10
**Figure 1.8** The monomer guest, host and polymer ..... 12
**Figure 1.9** Cocrystal of host and guest ..... 12
**Figure 1.10** Optimal geometry for diiododiacetylene polymerziatio ..... 14
**Figure 1.11** (A) Optical microscope image of bulk pyrrolidine-treated PIDA. Scale bars: 1 mm. (B) TEM image of pyrrolidine-treated PIDA dispersed in methanol. Scale bar: 500 nm. ..... 15
**Figure 2.1** Different oxalyl bearing hosts used for successful diacetylene topochemical polymerization ..... 18
**Figure 2.2** Positions on pyrydine for potential structure ..... 19
**Figure 2.3** Increased solubility of bis-urea macrocycle with PEG segment ..... 20
**Figure 2.4** Schematic drawing showing the arrangement of macrocyclic host with diiodo-monomer . 20
**Figure 2.5** Prototype of macrocycle host ..... 21
**Figure 2.6** Illustration of N-N distance on the macrocyclic host ..... 22
**Figure 2.7** The macrocyclic host ..... 25
**Figure 2.8** Conformers of the macrocycle of n=2 with PEG ..... 26
**Figure 2.9** Conformers of the macrocycle of n=3 with PEG..... 27
**Figure 2.10** Conformer with lowest energy (based on molecular mechanics and HF) ..... 28
**Figure 2.11** $^{13}C$ NMR spectrum of 1,4-phthalazinedione and phthalic diamide ..... 36

## List of Schemes

**Scheme 2.1** Proposed mechanism to approach carbyne ..... 17
**Scheme 2.2** The whole synthesis roadmap ..... 30
**Scheme 2.3** Functionalization on para site of 2,6-dibromopyridine ..... 31
**Scheme 2.4** Functionalization on 4-pentyne-1-ol and Sonogashira coupling ..... 33
**Scheme 2.5** Convert phthalimido into amino ..... 34
**Scheme 2.6** Model reaction using pentynyl-phthalimide ..... 37
**Scheme 2.7** Conversion of the phthalimido group into amine on compound **8** ..... 37
**Scheme 2.8** The synthesis of compound **14** ..... 40
**Scheme 2.9** Sonogashira coupling of compound **5** and **15** ..... 41
**Scheme 2.10** Alternative route by Boc protection ..... 42
**Scheme 2.11** Boc protection on 1-aminopent-4-yne ..... 42
**Scheme 2.12** Sonogashira coupling of **5** and **15** ..... 43
**Scheme 2.13** Future alternative route ..... 44
**Scheme 2.14** Copper-free Sonogashira formula ..... 44

## List of Tables

**Table 2.1** N-N distance of different hosts ( Equilibrium Conformer ) ..... 26
**Table 2.2** N-N distance of different hosts ..... 28

**Acknowledgments**

I would like to express my sincere gratefulness to my advisor, Prof. Nancy Goroff. I started my project with almost no background, but Prof. Goroff gave me great help and caring not just in my research but also my feeling because she knew that people suffer high pressure as a beginner especially where other coworkers are all aces. Besides the knowledge I have learned in lab, she really help me to understand how to be a team worker, how to maximize the efficiency of a group. As a result, I understand the true meaning of team spirit.

Thanks to all group members, without them, I can not have such good progress in a short time. It is a great pleasure to work with this lovely group. Thanks to my committee member, Prof. Lauher and Prof. Rudick, you gave me great help for my thesis and presentation. Thanks to this great department, it offers me this great chance to learn, to happily live in beautiful Stony Brook.

Many thanks to my friends, they company me when I felt sad, lonely and disappointed. I am very moved that they always try to keep my warm and positive. Special thanks to my soul mate Rose, words can not express my feelings, but I know you can feel it.

Finally, I would express my greatest thank to my parents. Thousands of minutes phone call across the Pacific Ocean, days and nights they always encourage me, happiness and tear they share with me. I love you!

# Chapter 1. Introduction

## 1.1 Conjugated Organic Polymers and Its Important Branch: Polydiacetylenes

When you are reading this report on your computer, billions of calculations are performed in a tiny silicon-based CPU so that billions of electrons are transported every second. The invention and application of silicon semiconductors have brought this world into a wonderful era, since more and more research is carried out by computers, it is urgent that a faster CPU is developed to assist the work such as calculation and modeling. Eversince scientists have found that the electron flow rate in a graphene transistor is 10 times faster than in silicon, graphene has been a target for transistors ins the future.[1]

After $C_{60}$ (buckminsterfullerene) was discovered in 1985 by Curl, Kroto and coworkers,[2] numerous carbon allotropes, like carbon nanotubes and fullerenes.[3] These carbon-rich materials have demonstrated fascinating electronic and optical properties which could potentially be applied to field-effect transistors,[4] organic light-emitting diodes (OLEDs),[5] photovoltaic cells,[6] chemical and biological sensors, and the next generation CPU-carbon chip.

Among carbon-rich materials, conjugated polymers are important for their conducting properties. The large scale $\pi$-electron delocalization through the whole conjugated backbone makes the conjugated organic polymer a conducting tube for electrons on a molecular level. Figure 1.1 shows representative conjugated polymers. Since the need for energy source is the major concern in the 21$^{st}$ century, conjugated polymers have stimulated huge research interests for their superb electronic and optical properties.

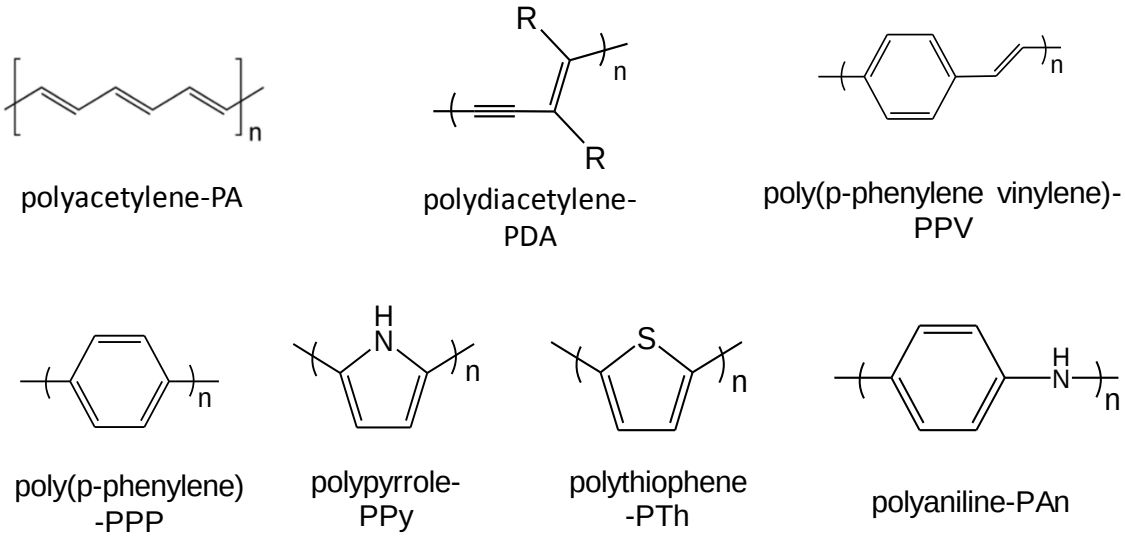


**Figure 1.1** Representative conjugated polymers

Polyynes are a branch of conjugated materials with linear structure and alternating carbon-carbon single and triple bonds. The longest polyyne, synthesized by Rik R. Tykwinski and Wesley Chalifoux in 2010, has 22 acetylenic units end-capped with triisopropylsilyl groups.[7] The polyyne with infinite repeating units is called carbyne, which has not been synthesized to date despite numerous efforts.[8] Figure 1.2 shows the structure of polyyne and carbyne.

**Figure 1.2** Polyyne and carbyne

Two of the most famous all-carbon materials are diamond and graphite, diamond consists of $sp^3$-hybridized carbon which is bonded with other neighboring carbons in 3 dimensional space, while graphite is composed of $sp^2$-hybridized carbon planarly bonded in 2 dimensional space. Carbon exists in three valence states of hybridization: $sp^3$, $sp^2$ and sp. As a result it is logical to

speculate an all-carbon material that consiste of only sp-hybridized carbon atoms linearly bonded in 1-dimensional space. This would be carbyne. Carbyne has triggered a great number of researchers to attempt its synthesis. The electrical and optical properties of conducting materials are heavily dependent on the way that carbon bonds:$sp^3$-hybridized diamond with only single bonds is an insulator, $sp^2$-hybridized graphite with single and double bonds is a semiconductor, so we are eager to know how sp-hybridized carbyne with alternating single and triple bonds behaves.

There are multiple methods to obtain polyynes,[9] such as oxidative dehydropolycondensation of acetylene, polycondensation of carbon suboxide with bis(bromomagnesium) acetylide, dehydrogenation of polyacetylene, plasma synthesis, laser-induced sublimation of carbon, etc. These methods can be roughly classified into two strategies: the homo- or hetero-coupling of preformed acetylenic precursors, and the elimination of side groups of preformed polymer. One of the most convenient ways is dehydrohalogenation of polymers, shown in Figure 1.3. The successful synthesis is largely dependent on full dehydrohalogenation with retention of the linear structure. Polyacetylenes with halogen substituents are potentially good precursors for carbyne synthesis through dehydrohalogenation. What is more polydiacetylene has higher carbon: heteroatom ratio so it is also a good model for inherent properties investigation. As a result the research of polydiacetylene and its dehalogenation is meaningful.

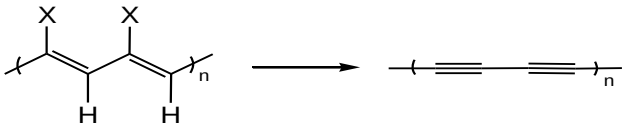


**Figure 1.3** Dehydrohalogenation of polymers

## 1.2 Topochemical Polymerization

Since PDAs are valued targets for the investigation of conjugated systems, great efforts are devoted to their synthesis. Diynes, like diiodobutadiyne, have 4 sp-hybridized carbons for chain propagation, which makes polymerization a very complicated transformation. Among all possible polymerization routes however, only 1, 4-polymerization can present the desired polydiacetylene. Traditional synthetic methods have low degrees of polymerization to prepare PDAs. For example in 1986 Wudl and Bitler[10] used palladium and nickel catalysts, but the degree of polymerization was only 7 (characterized by IR, $^{1}H$ and $^{13}C$ NMR and elemental analysis). However they showed that the functions of diynes' end groups do not just affect the synthetic procedures, but also the properties of the oligomers'.

Compared to all other synthetic strategies for making PDAs, topochemical polymerization is a good route. In 1969 Wegner[11] first observed diacetylene topochemical polymerization of 2,4-hexadiyn-1,6-diol derivatives in the solid state. Soon after Baughman[12] described the ideal diyne spacing geometry, the repeat distance between monomers should be equal to the repeat length in the polymer; for diynes this value is around 4.9 Å. The C1 to C4' distance in which the reaction occurs, should be brought within van der Waals contact range (around 3.5 Å), and there should be a 45 ° tilt angle between the axis of the monomer array and the monomer rod. These three spatial parameters facilitate the maintenance of the crystal structure in polymerization. However, this geometry does not work for all diyne polymerizations. There may be numerous reasons that could make the polymerization fail, for instance if the monomers can not crystallize on their own into a suitable spatial array, polymerization can not be triggered.

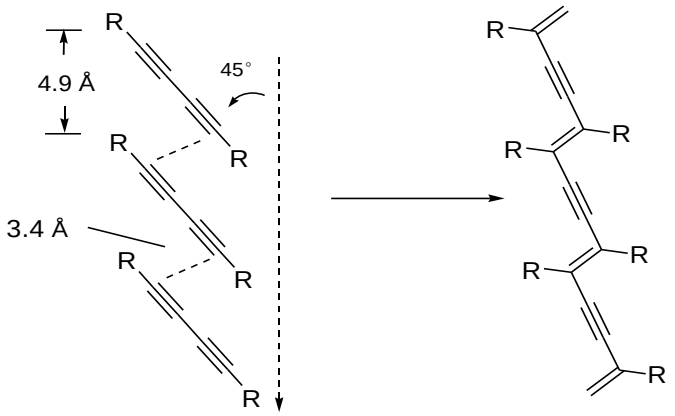


**Figure 1.4** Geometry for 1,4 polymerization of diacetylene

Some representative features of topochemical polymerization are shown in a simplified Figure 1.4: the monomer rotation at a specific angle is the key step to triggering the 1,4-polymerization with the neighboring monomer. The diacetylene topochemical polymerization is a single phase process. As a result of this single phase transformation, the polymers have exceptionally high purity and stereochemical regularity so that PDA crystals prepared by this method are suitable for the investigation of their inherent optical and electronic properties.[13] Figure 1.5 shows the spatial movement of monomers in topochemical polymerization.

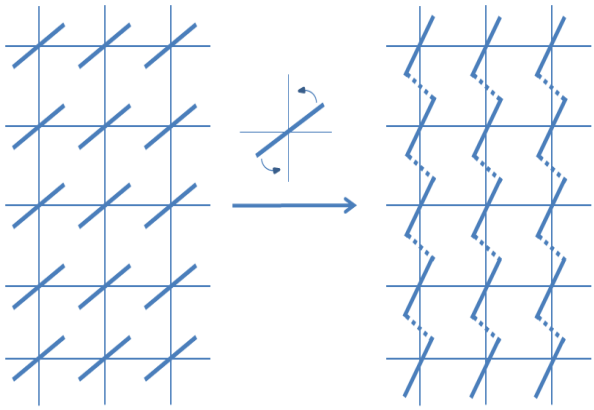

**Figure 1.5** Spatial movement illustration of topochemical polymerization: a monomer single crystal transforms into the polymer single crystal. Figure 1.5 is based on Figure 1 in Reference 13

## 1.3 Host-Guest Strategy

Since in many cases crystallization of monomers can not provide suitable crystal structure for topochemical polymerization, scientists began to develop strategies to control crystal structure based on the ideal geometry parameters. In order to control the structure, there must be some available forces that can be utilized to manipulate monomers, like covalent forces, non-covalent forces, static forces (ionic interaction), hydrogen bonds, van der Waals forces and π–π stacking. Hydrogen bonds are used in nature to organize molecules in the solid state specifically for molecular crystals and biopolymers including ice, cellulose and DNA. As a result, it is quite logical that scientists could utilize this persistent intermolecular force to design highly organized crystals in the solid state.

The first report of host-guest complexes was in 1967, when Pedersen studied alkali metal ions that bind to crown ethers and form a highly structured complex.[14] Expanded by Cram and coworkers[15] afterwards, host-guest chemistry has been developed into a broad field and is a good example of simulation from the interaction between substrate and enzyme.

### 1.3.1 The Self-Assembling of Host

There are several parameters that need to be considered in host-guest chemistry:

The first is the strength of the interaction between the host and the guest, but not strong enough to restrict movement during polymerization.[16] The second requirement for the host-guest chemistry is the packing geometry. Among all the geometric parameters, the monomer repeat

distance is the key parameter. This distance is governed by the repeat distance of the self-assembled host array.[13]

Figure 1.6 shows the repeat distances of different hosts. For diacetylene packing geometry, ureas and oxalamides are considered good candidates because the repeat distance of their self-assembled network is around 4.9 Å, and it is possible to add side groups on both sides of the urea or oxalyl segment. [17]

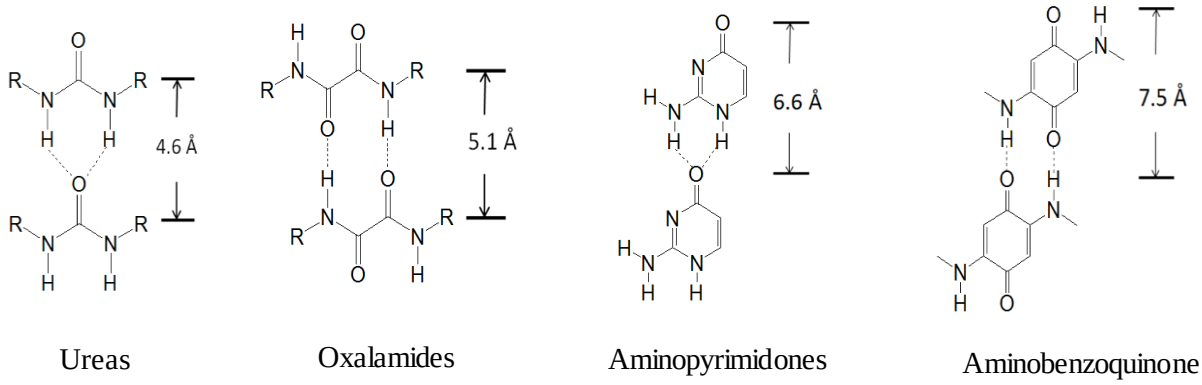


**Figure 1.6** Host that self-assembled into hydrogen bonding networks.[17] Figure 1.6 is based on Figure 2 in Reference 17.

Ureas have two hydrogen donors and one carbonyl acceptor, where the carbonyl acceptor can accept two hydrogen bonds at its lone pair position.[18] The oxamides are diamides of oxalic acid. Disubstituted oxamides with the same substituents on both sides can form an α-network, in which each carbonyl oxygen receives one hydrogen bond[19].

With the aid of the selected host, the monomer packing geometry can be predicted to a higher extent to increase the likelihood of successful reaction. This strategy uses synthetic chemistry, structural chemistry and crystal engineering to design a suitable host to interact with the monomers.

### 1.3.2 Host Guest Interactions

The interaction between the host and the guest should be strong enough for them to bind to each other. Figure 1.7 indicates some acid-base interaction. For example the carboxylic acid can form a hydrogen bond with pyridine because pyridine is Lewis basic. Alkynes are weakly acidic, the pKa of alkynyl protons is around 25, far more acidic than alkenes (50) and alkanes (40). Though the interaction of pyridine with a terminal alkyne is weak, it is still not negligible.

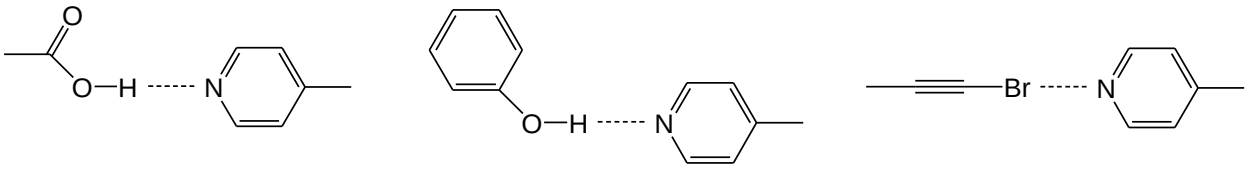


**Figure 1.7** Diverse acid-base intermolecular interactions of pyridines

Besides the conventional hydrogen-bonding interaction, there is another kind of weak interaction which has been used for arranging molecules: the halogen bond. Halogen bonding is a non-covalent interaction similar to hydrogen bonding. The role of halogen bonding is analogous to the hydrogen of hydrogen bonding, in which the halogen is Lewis acidic and interacts with Lewis a base like oxygen or nitrogen. [20]

In halogen bonding, the increasing electronegativity of both the donor and especially the accepter strengthens the bond. The strength order of halogen bonding is Cl < Br < I because of the increasing polarizability and decreasing electronegativity of the halogen. The hybridization of the carbon bonded to the halogen also affects the halogen bonding strength with the general trend C(sp)-X > C($sp^2$)-X > C($sp^3$)-X. Therefore haloalkynes are good halogen bonding donors. [20]

Another character of halogen bonding is the bond direction, which adds a new function of crystal engineering control to manipulate the geometry. The angle of noncovalent interactions of halogen atoms depends on the accepter's electronegativity. For electrophiles like metal ions, a smaller bond angle of 90-120 °is observed. For nucleophiles like oxygen and nitrogen this angle is generally 160-180 °.[20] This rule only works for Cl, Br and I. The definition of halogen bonding comes from the latter interaction: a near-linear bond angle with nucleophiles.

The question of whether or not there is a competition bwtween halogen and hydrogen bonding has investigated by Sandorfy and coworks[21]. Monitored by IR, they studied a series of organic base solutions that showed that the IR peak related to the solute-solute intermolecular hydrogen bond decreases upon the introduction of another solute which can primarily form halogen bonding. The order of increasing hydrogen bonding breaking potency is F < Cl < Br < I. Though they tested this rule and proved the existence of competition, for the halogen bond that forms with other halogen bonding donor the strength of this competition still depends. But their work gives us a good hint: the selection of appropriate halogen bonding donor acceptor pair is important to keep the integrity of hydrogen bonding network for host self-assembly.

### 1.3.3 Polydiiododiacetylene

An excellent example of the utilization of both halogen bonding and topochemical polymerization is the polymerization of diiodobutadiyne. Goroff and coworkers[22] used diiodobutadiyne as the guest monomer and different kinds of bisnitrile or bispyridyl oxalamides as the hosts to prepare cocrystals, followed by polymerization of monomer at room temperature.

The monomer, host and polymer are shown in Figure 1.8. The polymer they formed was polydiiodobutadiyne (PIDA), which has the simplest side grop of any polydiacetylene.

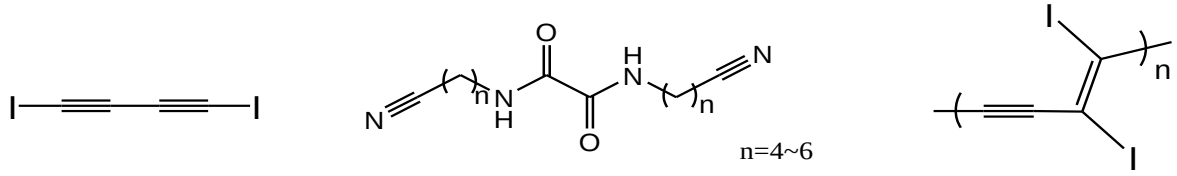


Diiododiacetylene Bisnitrile oxalamides PIDA

**Figure 1.8** The monomer, host and polymer

Iodine has high polarizability and low electronegativity, it is a good candidate for forming halogen bonds. What is more, if iodine is bonded to an sp-hybridized carbon, the increased electronegativity of carbon (compared to $sp^2$ and $sp^3$ hybridized carbon) will enhance the polarization to draw the C-X bond more towards carbon, resulting in a partially positive iodine, a suitable condition to form a halogen bond with Lewis bases.

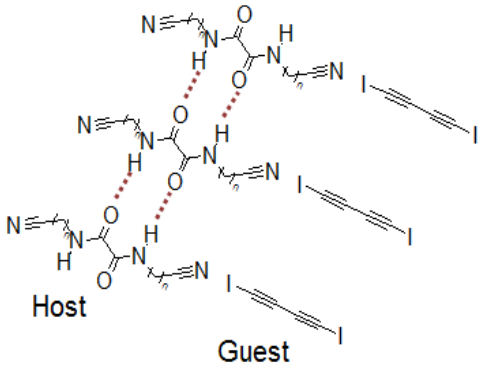


**Figure 1.9** Cocrystal of host

The preparation of co-crystals began with the solution of both host and guest in methanol in a 1:2 host-guest ratio. Slow solvent evaporation presented shining, metallic-looking cocrystal, Figure 1.9 shows its structure . With the interaction of the self-assembled host, the monomers are prearranged into the optimal alignment for topochemical polymerization: 4.9 Å repeat distance,

3.4Å C1-C4' distance, 45 °tilt angle between the axis of monomer array and monomer rod, shown in Figure 1.10.[23]

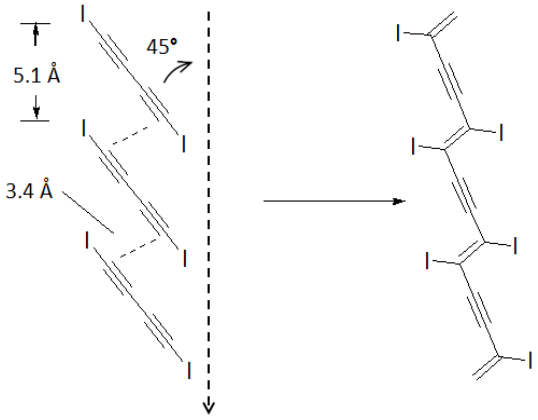


**Figure 1.10** Optimal geometry for diiodobutadiyne polymerization

During storage at room temperature the cocrystal appearance undergoes a transition from opaque blue to highly reflective copper color directly, simultaneously accompanied transformation to PIDA cocrystals. Multiple methods of characterization have been used to confirm PIDA formation and 50% conversion percentage from monomer to polymer.[23]

### 1.3.4 Dehalogenation of PIDA

After the successful preparation of PIDA, Luo and coworkers[24] tried to remove the iodine from PIDA. PIDA was first isolated from the cocrystal, and then dispersed PIDA nanofibers in organic solvents like tetrahydrofuran or methanol with sonication to present a blue suspension. After the addition of Lewis bases such as pyrrolidine, pyridine or triethylamine, the blue color disappeared. Stronger base causes a faster color change. Treatment with $Na_2S_2O_3$ on the resulting supernatant solution of the reaction between PIDA and neat pyridine indicated that molecular iodine was formed during the reaction. In methanol, the reaction between PIDA and excess pyrrolidine produces iodide, confirmed by the generation of yellow precipitate with the addition of $AgNO_3$. Figure 1.11 shows the optical microscope and TEM image of pyrrolidine-treated PIDA.

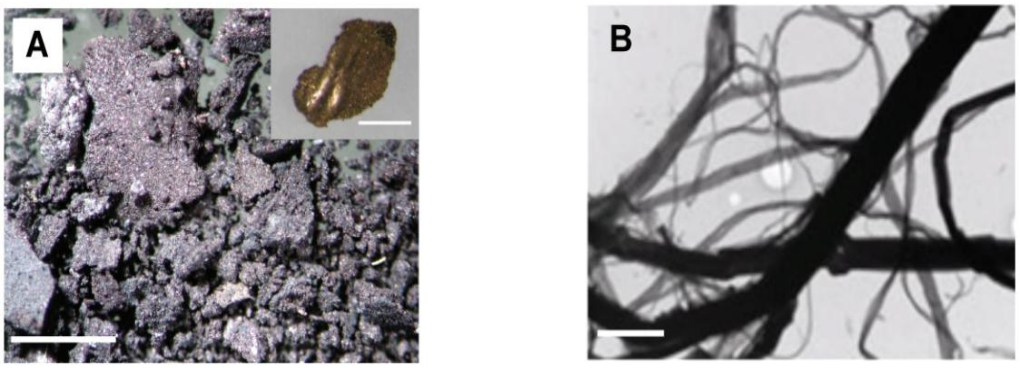


**Figure 1.11** (A) Optical microscope image of bulk pyrrolidine-treated PIDA. Scale bars: 1 mm. (B) TEM image of pyrrolidine-treated PIDA dispersed in methanol. Scale bar: 500 nm.[24] Reprinted (Figure 1.11) with permission from Reference 24. Copyright (2011) American Chemical Society.

Elemental analysis of base-treated PIDA showed that the carbon/iodine ratio increased to 7:1, compared to 2:1 of PIDA. Further dehalogenation is hindered because the interiors of insoluble PIDA aggregates are not accessible to base, meaning that iodine on PIDA is not exposed to base treatment, also as the dehalogenation progresses, the polymer chains may

contract or fold to make some iodine blocked from the outside. Additionally, cross-linking reactions between strands could also be occurring. Due to the fact that bulk PIDA can not be fully dehalogenated, a new strategy needed to be developed.

# Chapter 2. Discussion and Results

## 2.1 Host Design

The preparation of carbyne is hindered by partial dehalogenation, chains aggregation, and cross-linking reactions. Partial dehalogenation is a key problem and the reason is that not all iodine is accessible to base. Therefore, several problems need to be solved: (1) During the dispersion of PIDA in solvent, each PIDA strand should be kept extended to make all iodine accessible to base, rather than self-entangled to hide iodine inside; (2) During the dispersion of PIDA in solvent, each PIDA strand should be kept separated from the neighboring chains to prevent aggregation which may bury the iodine inside the aggregation. It is the intermolecular iodine crowding; (3) During the dehalogenation process, the previously isolated strands should still be separated to avoid aggregation. More importantly, the strand separation during dehalogenation can also avoid chemical interaction between strands (i.e. cross-liking), not only physical aggregation.

Such requirements can be met by using a hollow tubular framework structure to contain the PIDA strand inside. The monomer diiodobutadiyne should be able to polymerize inside. The most suitable method to prepare PIDA is to use topochemical polymerization based on the host-guest strategy, therefore all requirements of this method should be fulfilled: The tubular framework can be prepared either by self-assembling or other intermolecular interaction like $\pi$-$\pi$ stacking. Second, the inner space of the tubular framework should be big enough to accommodate the monomer inside. Last, the monomer should be aligned into a specific spatial arrangement. What is more, there must be a binding site on the framework to interact with monomers for alignment. Last, there must be a way for the tubular framework to interact with the

monomer. In this case, solvent is a good medium for the interaction. Hence, the tubular framework and the monomer need have good solubility in the same solvent.

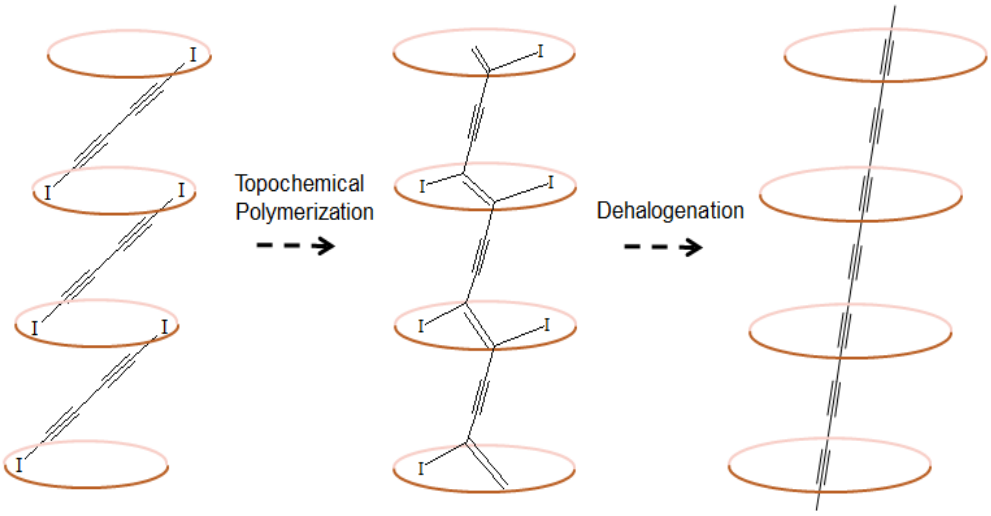


**Scheme 2.1** Proposed for carbyne preparation

### 2.1.1 Design for Self-assembling Function

The repeat distance of the self-assembled host primarily determines the monomer repeat distance. Among all host candidates, the repeat distance of the host with oxalyl segment is near 4.9Å and it is the close to the geometry requirement of PDA topochemical polymerization. Multiple successful cases have been reported to use topochemical polymerization to prepare different polydiacetylenes using oxalyl bearing host (shown in Figure 2.1). What is more, both sides of the oxalyl group could be connected to different segments therefore oxalyl can be used to prepare versatile hosts with different functions. [22]

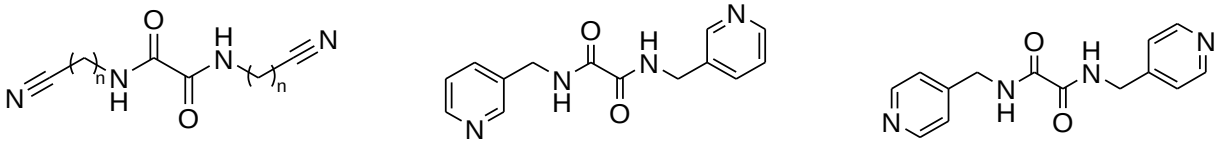

**Figure 2.1** Different oxalyl bearing hosts used for successful diacetylene topochemical polymerization

### 2.1.2 Design for Host-guest Interaction

In order to have desirable host-guest interaction, the most important problem is to select suitable halogen bonding donor accepter pair. First the atom bonded on either hydrogen bonding donor or halogen bonding donor should be able to form reliable either hydrogen bond of halogen bond, it requires that this atom could be easily polarized so that it can be partially positive. Second the hydrogen bond / halogen bond accepter should be basic enough to provide electron pair. Fowler, Lauher and coworkers[25] found that if the pKa difference between H/X and accepter is too large, it will induce proton transfer which will cause the formation of ionic interaction rather than non-covalent bond even in solid state (proton transfer is easier in solution).

Goroff and coworkers[23] have used pyridines and nitriles to prepare host-guest complexes with diiodobutadiyne with successful polymerization afterwards. Figure 2.2 shows the 2,3,4,5, and 6 positions of pyridine can be used to connect versatile segments to prepare cyclic structures. Thus, the iodine-substituted diyne and pyridine make a good halogen bonding donor/accepter pair for host-guest interaction.

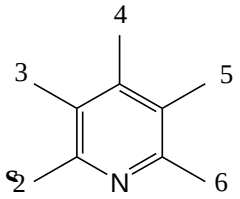


**Figure 2.2** Positions on pyridine for attachment

### 2.1.3 Adjustment for Solubility and Ring Flexibility

Base on the experiences of Shimizu and coworkers[26], macrocyclic structures usually suffer low solubility. As mentioned above, in order to have the interaction of host and guest, there must be a medium for them to interact and it is usually a suitable solvent. Shimizu and coworkers[26] demonstrated that polyethylene glycol (PEG) segments can increase the solubility of organic compounds. An example trend is shown in Figure 2.3. The flexible structure is the reason why the self-assembled complexes will not form a neat packed column, but will instead form complicated complexes with zigzag and/or staggered shape.

As a result, a rigid segment may be helpful to limit the conformations of the macrocycle.

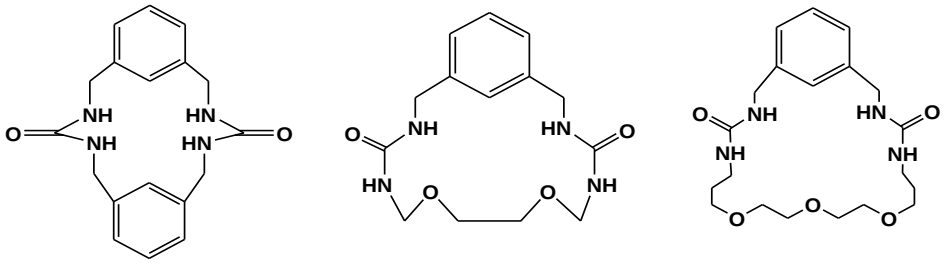

**Figure 2.3** Increased solubility of bis-urea macrocycle with PEG segment[26]

### 2.1.4 Geometry Calculation

Calculations were performed to determine parameters for packing of diiodobutadiyne inside a macrocyclic host. Shown in Figure 2.4, the length of diiodobutadiyne is 7.9 Å (measured on Spartan), the gap between the nitrogen of the pyridyl and the iodine of the monomer is 3.2 Å. Based on the packing geometry of diiodobutadiyne, the distance between two on opposite sides in one macrocyclic host should be larger than (3.2 ×2) + 5.6 =12 Å. Even though modeling does not precisely predict the real situation, it is still good reference for our designing.

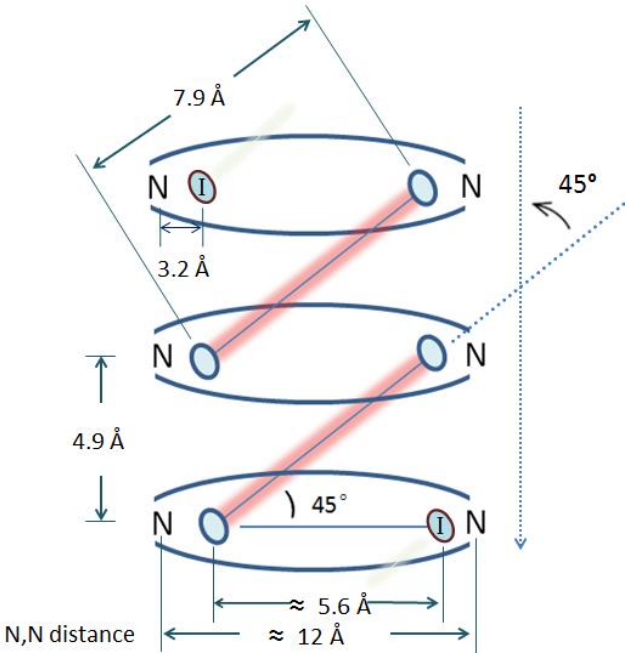


**Figure 2.4** Schematic drawing showing the arrangement of macrocyclic host with diiodobutadiyne

After considering all problems above, the first prototype of the macrocyclic host is shown in Figure 2.5. It has oxalamide segments for self-assembling, pyridine segments for host-guest interaction, and PEG for solubility increase. The next question to decide is the ring size.

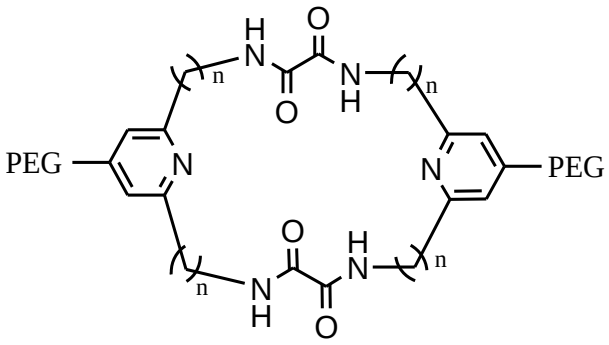


**Figure 2.5** Prototype of macrocycle host

## 2.2 Computational Simulation of Conformation

### 2.2.1 General Introduction of Computational Modeling[27]

Computational modeling provides a convenient method to predict many different properties of chemical compounds before the synthesis in the laboratory. The conformation of the macrocyclic host is the key parameter because of the need to accommodate the guest molecule diiodobutadiyne into the internal tubular space of the self-assembled framework. The size of the host that needs to be considered is shown in Figure 2.6.

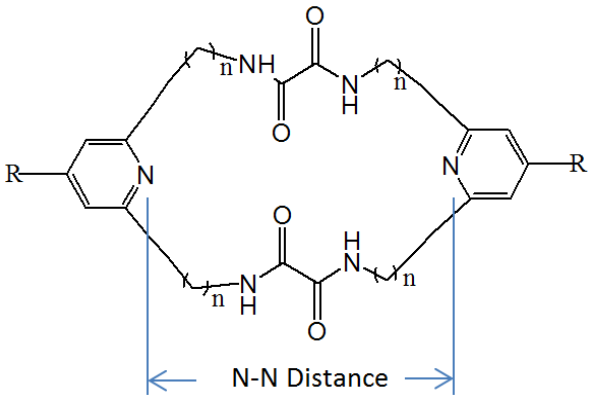


**Figure 2.6** Illustration of N-N distance on the macrocyclic host

As mentioned before, both size and "interior structure" of the tubular framework will directly affect whether or not the tubular framework can accommodate the guest, and also the geometry of the host-guest interaction. It can be predicted in solution or solid state the macrocyclic host will not exist in a flattened form, because it has multiple flexible single bonds which can adopt various conformations. Therefore, both the outer and the inner structure of the self-assembled tubular framework can not be predicted and described base on the flattened form.

What is more, the preparation of host-guest complex will be conducted in a solvent, and the inter- and intra-molecular interactions of host-guest complex depend on the type of solvent.

If some estimation of the macrocyclic host's conformation can be extracted from computational modeling, the interaction between the host and guest can be partially predicted. As a result, the computational modeling can not only predict the likelihood of the interaction, but also the interaction way host-guest complex may adopt. Though the modeling is not completely accurate, compare to the real condition, it could provide information to predict possible results.

### 2.2.2 Basic Level Molecular Mechanics Calculation

The force field, in terms of molecular modeling, is a set of parameters and forms of mathematical functions used to describe the potential energy of particles (typically molecules and atoms). The parameters include equilibrium bond lengths, bond angles, partial charge values, force constants, van der Waals etc. Different force fields use different mathematical expressions and parameters to describe potential energies of a certain systems. Most force fields were developed either from experimental data and/or higher level quantum mechanical calculations.[28]

Selecting the right force field will not only present good result but also it will save time. Under the molecular mechanics model, the simplest are SYBYL (Tripos, Inc.) and MMFF (Merck Molecular Force Field). When applying molecular mechanics models, both are suitable for determining equilibrium geometries and conformations. SYBYL can be applied throughout the entire periodic table. MMFF, developed by Merck Research Laboratories originally for drug design, is one of the most recently published force fields and has been proved suitable for the simulation of low-energy conformers and the diverse conformers libraries construction. (MMFFaq includes aqueous energy corrections). The molecular mechanics model combines simple algebraic equation for the energy of a compound described as "bonded atoms". These

basic algebraic equations describe various important parameters of a molecule. This model is fundamentally different compared to quantum chemical models which take no reference from chemical bonding. The assumption of molecular mechanics is based on the transferability of parameters from one molecule to another. As a result, this method enables a very simple calculation which can be utilized for complex molecular systems.[28] MMFF was chosen for modeling the macrocyclic host because it is very suitable for simple organic molecule (compare to complex biomolecule) for basic calculation.[28] MMFF also takes lot less time than higher level quantum mechanical calculation.

What is more, the calculation procedures recommended by most computational chemists (also recommended by Spartan operation manuals)[28] is to start with MMFF to obtain a list of low energy conformers, and then submit this list to desired higher level computational methods to perform the simulation with higher accuracy.

### 2.2.3 Equilibrium Conformers Using MMFF

Based on Spartan, the simulation could begin with a "quick view" function - <Equilibrium Conformer >, it is typically used to obtain a good guess of conformer with lowest energy because different force fields could be tested with simple but time-efficient calculation.

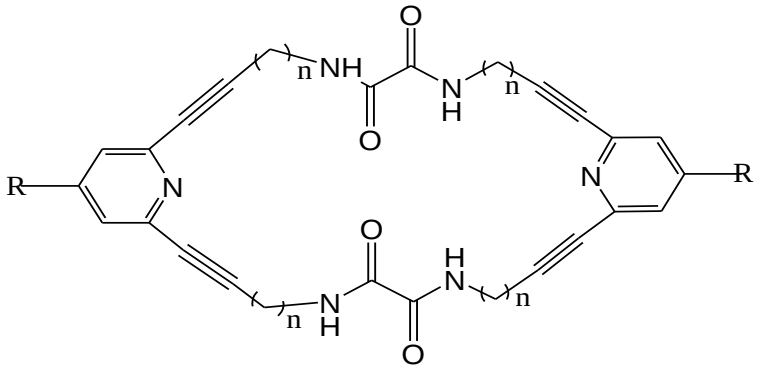


**Figure 2.7** The macrocyclic host

For the convenience of the discussion below, the C1-C2 bond is drawn as triple bond and three quarters of this host is semitransparent.

First, the relation of N-N distance and "n" number was analyzed from n=2 to n=4, while C1-C2 was set a single bond (Figure 2.7). Theoretically as n increases, N-N distance increases if the ring is flattened, however the ring size in the real case is not corresponding to n because the ring consists of multiple flexible single bonds, and therefore does not adopt a flattened conformation. Because the tubular framework can be formed only if the macrocyclic host adopts a relatively flattened shape, a C1-C2 triple bond was introduced. Surprisingly, the triple bond did not efficiently flatten the ring.

The PEG segment does not affect N-N distance in most cases (except n=4 with C1-C2 triple bond). (Table 2.1)

**Table 2.1** N-N distance of different hosts (Equilibrium Conformer)

| | C1-C2 single bond | C1-C2 single bond PEG | C1-C2 triple bond | C1-C2 triple bond PEG |
|---|---|---|---|---|
| n=2 | 10.119 | 10.189 | 4.827 | 4.731 |
| n=3 | 6.303 | 7.006 | 5.643 | 5.748 |
| n=4 | 9.010 | 10.143 | 10.693 | 7.752 |

Even though < Equilibrium Conformer > can enable us to view the conformer with the lowest energy with short calculation time, there is still a series of low energy conformers. Thus, it is necessary to perform a calculation to obtain a relatively long list of low-energy conformers, and a range of NN distances. Therefore, besides the < Equilibrium Conformer >, the <conformation distribution> is essential. [28]

Figure 2.8 shows the conformation difference with and without the introduction of the triple bond. This difference is especially obvious when n=2. When C1-C2 is single bond the macrocycle is more flattened than the macrocycle with C1-C2 as a triple bond.

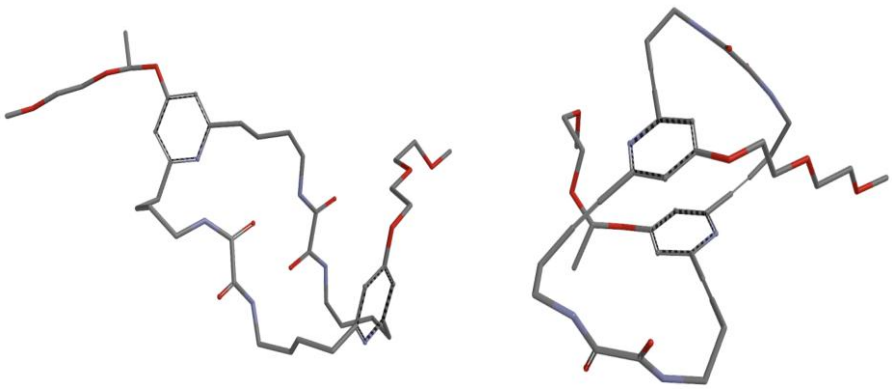

**Figure 2.8** Conformers of the macrocycle of n=2 with PEG.
(left: C1-C2 is a single bond; right: C1-C4 is a triple bond )

In Figure 2.9, the macrocycles with n=3 are less flattened compared to the macrocycle of n=2. What is more, the N-N distance of the macrocycles with C1-C2 as a single bond is slightly longer than the macrocycle with C1-C2 as a triple bond.

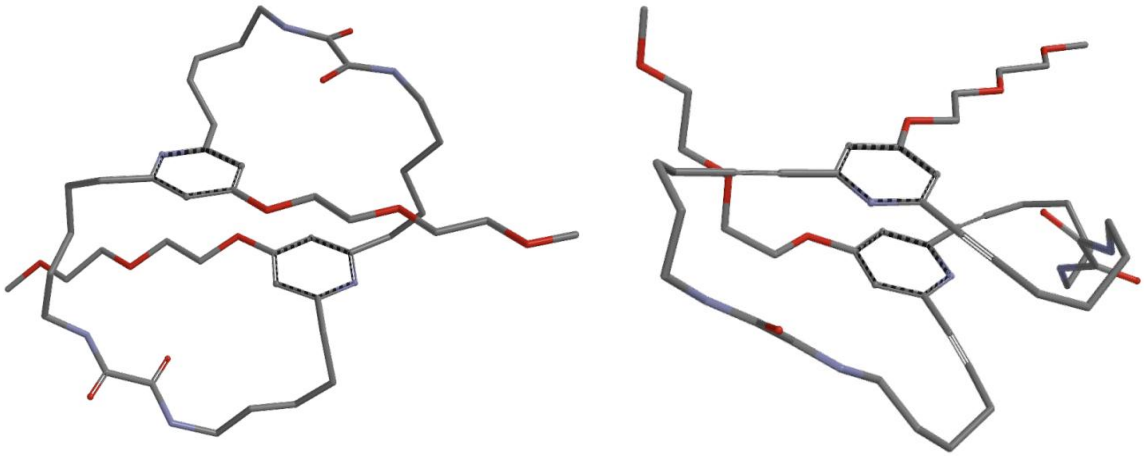

**Figure 2.9** Conformers of the macrocycle of n=3 with PEG. (left: C1-C2 is a single bond; right: C1-C4 is a triple bond )

## 2.2.4 Higher Level Quantum Chemical Calculation

After the majority of high energy conformers was sifted out by molecular mechanics model, the short list of low energy conformers was submitted to quantum chemical calculations.

One of the most common quantum chemical calculations is Hartree-Fock (HF) model (it is also called self-consistent field method-SCF), in which the primary approximation is central field approximation. This approximation for many-electron atoms considers the combined electric fields of the nucleus, and all the electrons which acting on any electrons are radial and identical to all other electrons in the atom. In this model the potential energy of the electrons is only a function of distance from the nucleus.

**Table 2.2** N-N distance of different macrocyclic host

| n | N-N Distance |
|---|---|
| 2 | 6.8-9.5 Å |
| 3 | 7.8-10.9 Å |
| 4 | 9.2-10.2 Å |

Based on the character of aforementioned models, HF was selected with 3-21G basis set (good balance between quality and CPU time). Since the macrocyclic host has not been synthesized, its solubility is unknown, so this calculation was conducted in (vacuum). The measured N-N distances are shown in Table 2.2. The conformer with the lowest energy is showed in Figure 2.10. As we can see from the picture, the macrocyclic host is not as flattened as we expected.

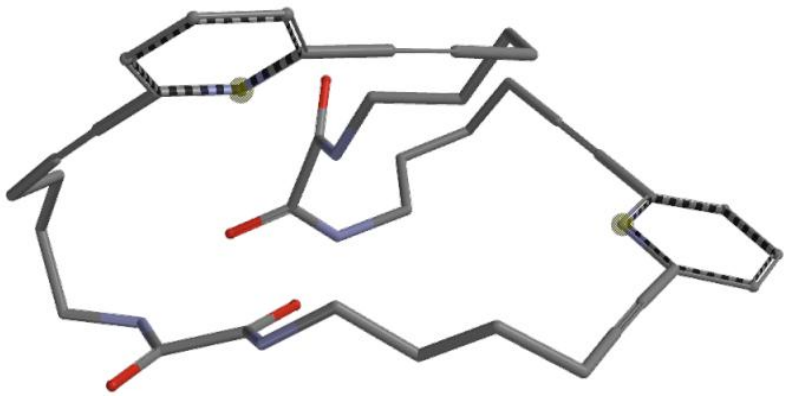

**Figure 2.10** Conformer with lowest energy (based on molecular mechanics and HF)

Base on the calculation data, the host which n=3 has N-N distance range from 7.8-10.9 Å, close to the desirable distance to accommodate the monomer. Therefore it was selected to begin the synthesis.

## 2.3 Synthesis

The macrocyclic host consists of four segments: PEG, pyridyl, alkynyl and oxalyl. The final product is symmetrical so the last step can be a ring-closure that combines two semicurclar components (**15** to **22**). The addition of an oxalyl segment to an alkynyl segment can be achieved using the reaction between an amino group and ethyl oxalyl chloride. Under low temperatures the amino group will only react with the chlorine side of ethyl oxalyl chloride (**9** to **15**),[39] at higher temperatures it can also react with the ethoxy side. The amino group on the alkynyl chain can be obtained through a Gabriel synthesis. The alkynyl chain can be attached to phthalimide via a Mitsunobu reaction (**6** to **7**).[32] In order to connect the alkynyl group to the pyridyl group, the Sonogashira coupling can be used to couple the hydrogen on the alkynyl group and the halogen on the aromatic ring (**5** & **7** to **8**).[33,34] Before the addition of PEG to the pyridyl segment, the functionalization on **4** position of pyridyl can be reached by direct hydroxylation (**1** to **2**).[29] After the tosylation of diethylene glycol monomethyl ether (**3** to **4**),[30] the PEG and the hydroxyl group on the pyridyl group can be connected under basic conditions (**2** & **4** to **5**).[31]

To sum up, the whole synthesis can start from the functionalization of 2,6 dibromopyridine, diethylene glycol monomethyl ether and 4-pentyne-1-ol. (Scheme 2.2)

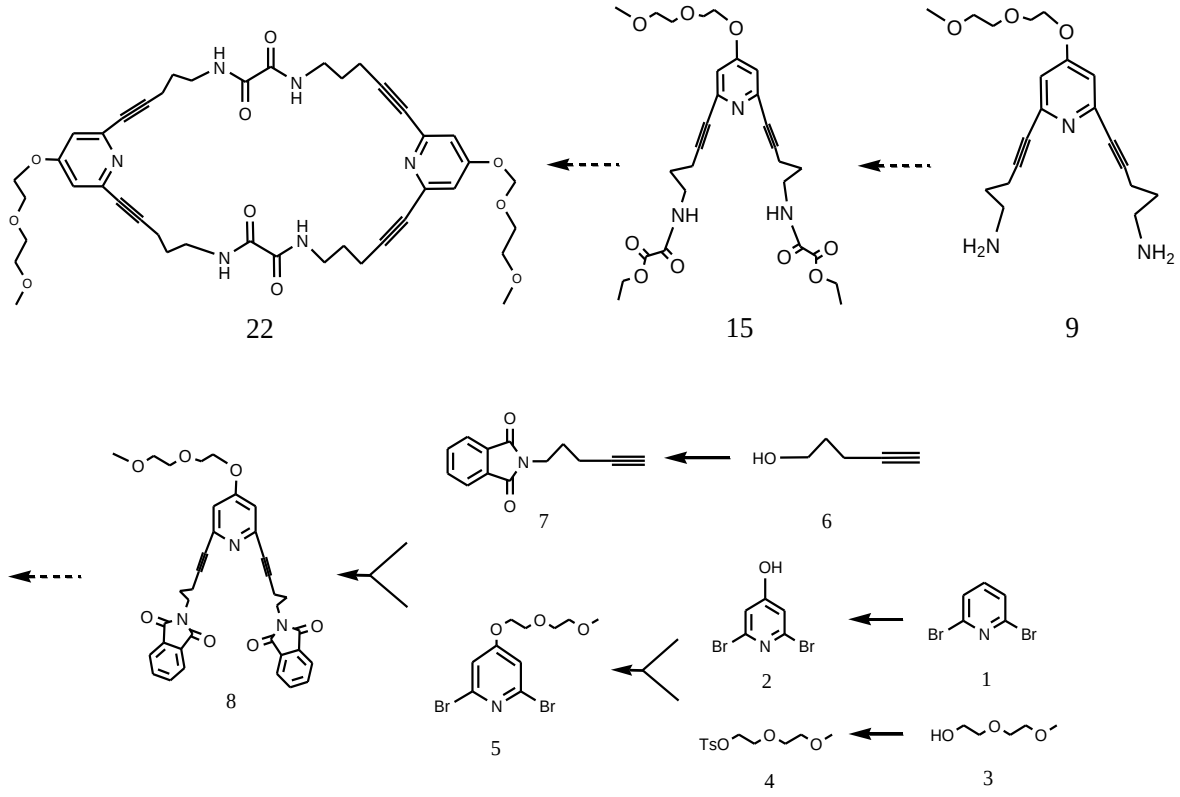


**Scheme.2.2** The whole synthesis roadmap

## 2.3.1 Functionalization on para Site of 2,6-Dibromopyridine

The synthesis begins with commercially available 2,6-dibromopyridine **1**.[29] The two bromines on the pyridine ring will be used for coupling with alkynyl chains, however there is no reactive site for connecting the PEG chain, so a new reactive site must be introduced.

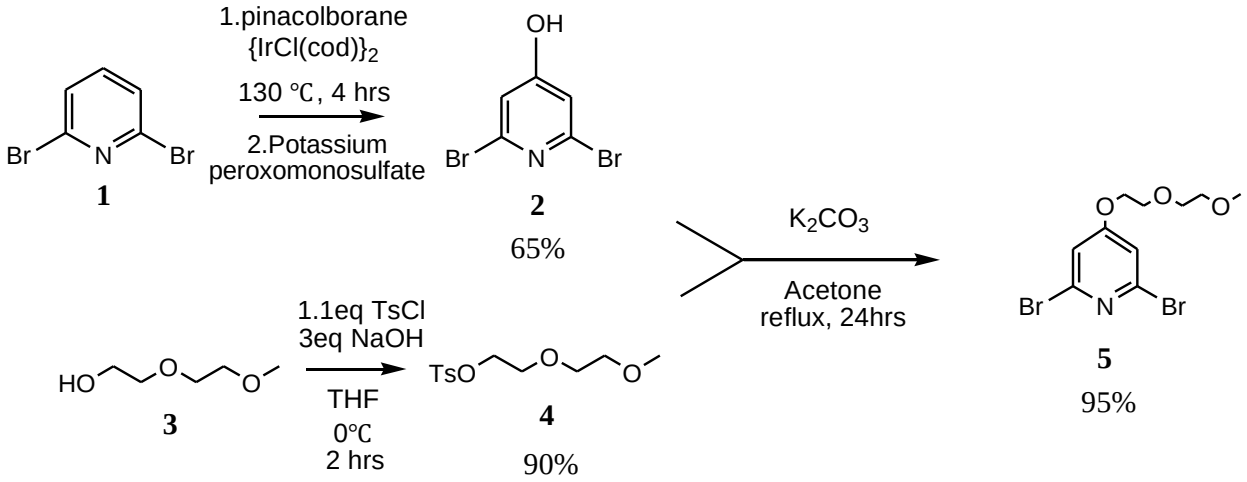


**Scheme 2.3** Functionalization on para site of 2,6-dibromopyridine[29, 30, 31]

According to Masahiko Inouye's work[29], the 2,6-dibromopyridine-4-ol **2** was synthesized by direct iridium-catalyzed borylation of 2,6-dibromopyridine **1**, followed by oxidation with Oxone (potassium peroxymonosulfate). Eight-years-old catalyst was used for the first attempt and it only gave low yield, approximately 25%. Doubling the catalyst amount or longer reaction time (even up to 24 hrs, 4 hrs for literature data) was not helpful to increase the yield. After using a brand new catalyst, the yield increased to 65%. The older catalyst had most likely partially decomposed.

The tosylation of diethylene glycol monomethyl ether **3** was straightforward according to literature report.[30] With the aid of NaOH, the reaction was driven towards the product with up to

90% yield in a short time. After extraction, and washing with water and brine, the product was pure enough for the next step even without column chromatography purification.

The tosyl group is a very good leaving group, so under basic conditions the nucleophile aryl oxide anion (the pyridinol deprotonated by carbonate) attacks the tosylate. Refluxe in acetone for 24 hours afforded dibromopyridine-PEG **5** as a pale yellow sticky oil.[31] (Scheme 2.3)

## 2.3.2 Functionalization on 4-Pentyne-1-ol and the Coupling with Pyridyl

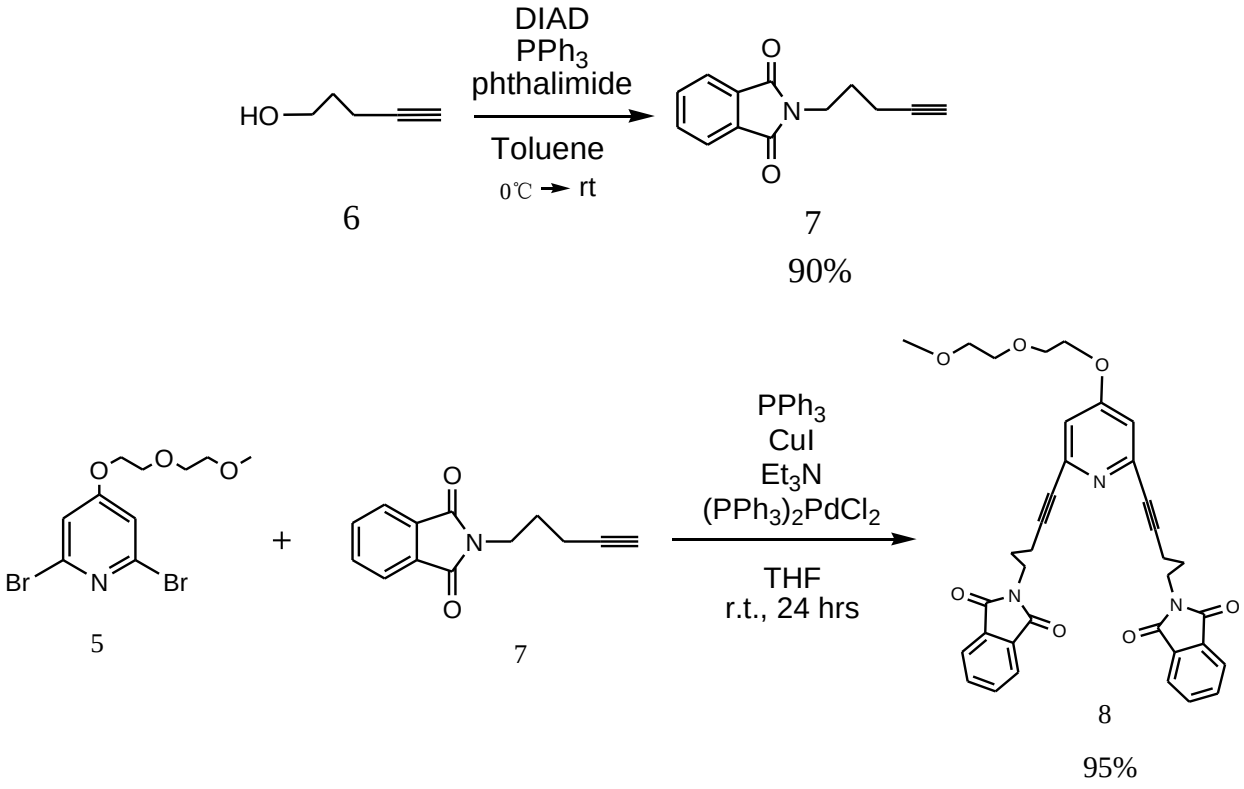


**Scheme 2.4** Functionalization of 4-pentyne-1-ol and Sonogashira coupling[32, 33, 34]

The two bromines on the pyridine ring and the ethynyl hydrogen of 4-pentyne-1-ol are used for Sonogashira coupling. [32] In the preparation of pentynyl-phthalimido **7**, according to the literature conditions for preparing similar compounds, different solvents and conditions were tested including anhydrous THF, 1:2 toluene:ethanol, and toluene. The use of THF and the toluene/ethanol mixture was not successful. For the conditions in toluene, the reaction was successful and the crude product was easy to purify. The product is colorless and crystalline at room temperature.

Because the molecular weight of pentynyl-phthalimido **7** is much higher than pentynyl-ol **6** and the percentage of pentynyl-phthalimido **7** in the crude product is usually as low as 30%, the purification had to be conducted on a large scale and was time-consuming. Recrystallization conditions were attempted. The solubility of pure pentynyl-phthalimido **7** in hexane was found to be very low, so hexane was used to dissolve the crude product. The insoluble solid and filtrate were separated by filtering and analyzed.

The crude product, a mixture of 1.5 g solid and oil was used for recrystallization. Based on the aforementioned impurity of the crude product, this amount contained about 450 mg pentynyl-phthalimido **7**. 20 mL Hexanes was used to dissolve the crude product, about 1 g solid residue was collected by filtering. TLC indicated that in the solid residue, one byproduct spot disappeared while the others remained; the filtrate had all byproduct and product spots. Since the TLC analysis with UV lamp is very sensitive to even trace amounts, the filtrate was purified by column chromatography to separate each component and calculate the percentage: From about 0.5 g material (among 1.5 g crude product) that dissolved in filtrate, the product was 97 mg taken about 20% weight percent, it also indicated that approximately another 300 mg was still contained in solid residue. The purity of the solid residue and filtrate were not enough to continue to the next step Sonogashira coupling, so that recrystallization was not applicable. Thus, traditional silica-gel column chromatography was still chosen for purification. Conclustion: the product was not pure by recrystallization so a column still had to be run.

Bis(pentynylphthalimido) **7** was used for Sonogashira coupling with dibromopyridine-PEG **5**.[33] An excessive of bis(pentynylphthalimido) **7** (2.3 equivalents**)** was used to guarantee the two bromine positions of dibromopyridine-PEG **5** would be coupled by bis(pentynylphthalimido) **7**, with 2.25 equivalents $Et_3N$ as base. However only 30% of dibromopyridine-PEG **5** (based on the

starting amount of dibromopyridine-PEG **5**) was disubstituted, another 30% of dibromopyridine-PEG **5** was monosubstituted. Further literature searching suggested that in some cases a higher ratio of terminal alkyne to aromatic halide is used (even up to 6:1 for disubstitution case) with more base.[34] Thus, 4 equivalents alkynyl component was added, using $Et_3N$ as both base and solvent. Since the mixture in neat $Et_3N$ was aggregatred, a cosolvent anhydrous THF was added at $Et_3N$/THF=1/1. Under the higher alkynyl:aromatic halide ratio of 4:1, almost quantitative yield of di-phthalimido-pyridine **8** was obtained. (Scheme 2.4)

## 2.3.3 The Preparation of 2,6-Di-2-(pent-4-ynyl)-1-amino-4-[2-(2-hydroxyethyloxy) ethyloxy]pyridine

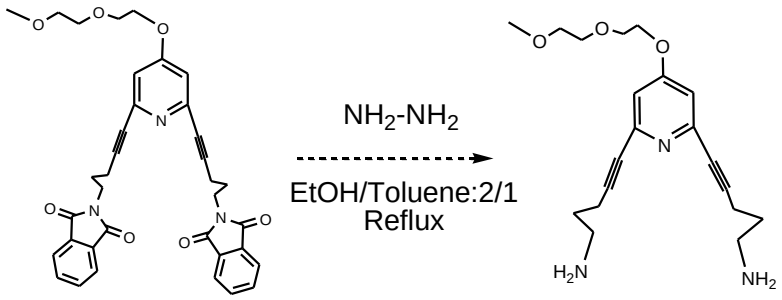


**Scheme 2.5** Conversion of the phthalimido group to the amine[34]

Hydrazine is a commonly used reagent to convert phthalimido into amino groups. Compound 8 (100 mg) was subjected to hydrazinolysis for first trial (Scheme 2.5). The resulting compound only showed two peaks in $^{13}C$ NMR spectrum in aromatic region: 128.56, 132.14. Surprisingly, the two peaks were the same as the portion that came after the product in column chromatography of the Sonogashira coupling product mixture. The portion the came after the product was yellow, no response observed under UV.

The $^{13}C$ NMR spectrum was compared to two possible byproducts shown in Figure 2.6: 2,3-dihydro-1,4-phthalazinedione (left)[35] and phthalic diamide (right)[36]. Neither of them corresponds to the product obtained. (Figure 2.11)

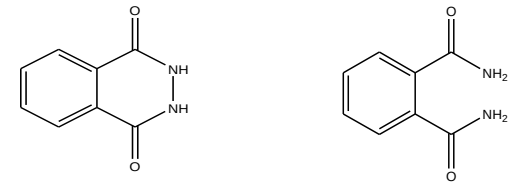


| $^{13}C$ NMR |
|---|
| 125.12 |
| 127.19 |
| 132.52 |
| 154.67 |

| $^{13}C$ NMR |
|---|
| 128.07 |
| 129.66 |
| 136.65 |
| 170.65 |

**Figure 2.11** $^{13}C$ NMR spectrum of 1,4-phthalazinedione and phthalic diamide[35]

Because this conversion was not successful on disubstituted pyridyl compound **8**, a trial on a smaller and simpler compound may provide important reference for this step.

Thus**,** pentynyl-phthalimido **7** was tested Gabriel synthesis for in order to choose suitable reaction conditions. Following the procedures of Guan (Scheme 2.6)[37]**,** the alkynyl amine was obtained as expected, using EtOH as solvent. Because the amine is very temperature sensitive, in the first trial the temperature of oil bath was set at 100 ℃, and the NMR spectrum had multiple peaks which did not belong to the product. The temperature of the oil bath may make a difference, because the solvent boiled when oil bath temperature is higher than its boiling point, the temperature of RBF wall may still very close to oil bath. As a result if the oil bath temperature is too high, it would bring negative effect on amine. Then the oil bath temperature was carefully adjusted to 70℃, and under these conditions very pure pentynyl-amine **10** was obtained. (Scheme 2.6)

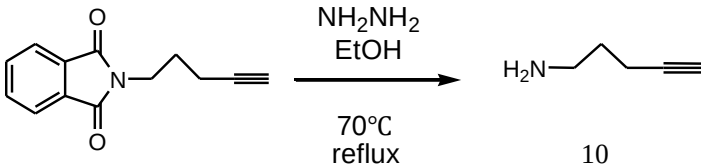


**Scheme 2.6** Model reaction using pentynyl-phthalimide 7[37]

The amount of solvent was also an issue. If the solvent was added according to the literature procedures, 10 minutes after the addition of hydrazine, a large amount of white precipitate formed and the magnetic stir bar could not disperse the mixture, so that extra solvent was added and a sonicator was used to disperse the aggregate. Learning from this experience, the solvent amount was tripled in the next trial which diluted the concentration of pentynyl-phthalimido **7**. The white precipitate still appeared about one hour later. The reaction was heated at reflux for 2 hours longer than before, but the yield decreased to 50%, lower than 70%.

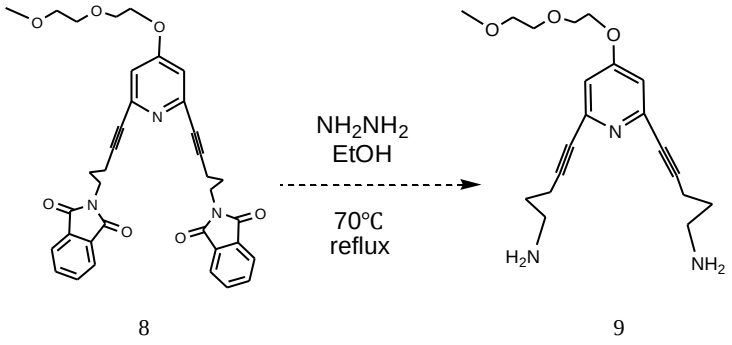


**Scheme 2.7** Conversion of the phthalimido group into amine on compound **8**[37]

Now that the conditions were optimized on pentynyl-phthalimido **7**, they were tested on di-phthalimido-pyridine **8 (**Scheme 2.7**)**. Dark orange **8** (316 mg, 0.5 mmol) was placed in 20 mL

EtOH, but the solubility was low, though the solvent did turn orange. After workup, a dark orange oil was obtained. The $^{13}C$ NMR spectrum showed that the reaction was not successful: only 2 peaks of the PEG segment were found at 70.6 and 71.7; the peaks of the pyridine ring were not identified. Sonication was applied to disperse the bulk but was unsuccessful. After purging with argon, the round bottom flask was immersed in a 70 ℃ oil bath, and 2 equivalents of hydrazine monohydrate were added. The solution became turbid at first, and precipitate was formed later. After 2 hours, the resulting mixture was an orange suspension. After it was cooled to room temperature, 10 mL water was added, and 5M HCl was used to acidify the solution in order to protonate the amine and make it water soluble. Followed by filtering, the acidic aqueous solution was clear dark orange. It was cooled down and kept at 0℃ in ice bath , basified with NaOH (aq) to pH=14, extracted with $CH_2Cl_2$ 30 mL × 5 times, dried over $MgSO_4$ and filtered. The organic layer was dark orange. (Note: The aqueous solution was still yellow even though the $CH_2Cl_2$ layer of last extraction was visually colorless.) Upon removal of solvent *in vacuo*, a sticky dark orange oil was obtained.

The purification of amines is difficult since some are unstable and their high polarity makes them hard to purify by silica chromatography. Additionally, since di-amine-pyridine **9** contains a pyridine ring and a PEG chain, it may still exist in the aqueous layer even pH14.

In the conversion from pentynyl-phthalimido **8** to pentynyl-amine **9**, the same purification method for purifying the crude product di-amine-pyridine **10** was used to purify the crude product of pentynyl-amine **9,** the resulting product was characterized on NMR. The $^{1}H$ NMR spectrum shows four peaks at δ3.2, 3.4, 3.5, 3.7 with same peak area, it clearly showed the PEG segment. The peaks at δ7.3, 7.5 may correspond to byproduct with aromatic ring (either 1,4-

phthalazinedione or phthalic diamide). The peak at δ 5.15 may correspond to proton of pyridine ring (the peak at δ 6.70 is the pyridine proton of tosyl-PEG **4**). Though the peaks of alkyl protons in the range from δ1-2.5 were shown, however their peak areas ratio is not in an appropriate proportion. For $^{13}C$ NMR spectrum, the peaks at δ 66, 69, 70, 71 may correspond to PEG carbon (δ 69, 70, 71, 73 are PEG carbon peaks for tosyl-PEG **4**). Either δ 53 or δ 58 may correspond to the methyl carbon of PEG. Several low height peaks within δ 17~38 may correspond to the alkyl segments, but their height ratio is also not in appropriate ratio.

Though purification procedures could purify the crude product of pentynyl-amine **10**, however when it was applied to crude product of di-amine-pyridine **9**, the NMR spectrum did not show clear evidence for the product.

Even though hydrazinolysis of pentynyl-phthalimido **7** was successful, when applied to di-phthalimido-pyridine 8, the NMR did not show sufficient evidence of product formation. Furthermore, the no-water purification was also successful with pentynyl-phthalimido **7** but formation of pentynyl-amine **9** was still not detected. As a result, a detouring route had to be developed.

## 2.3.4 Model Test for the Reaction of Pentynyl-amine 10 and Ethyl Oxalyl Chloride

Since pentynyl-amine **10** can be obtained with high purity in 70% yield, it can be used to react with ethyl oxalyl chloride. This reaction can be considered as a model test, also it may be a good way to use ethyl oxalyl chloride to protect the unstable and sensitive amino group first, pure **10** was used for this reaction and was ran very smoothly with high yield. (Scheme 2.8)

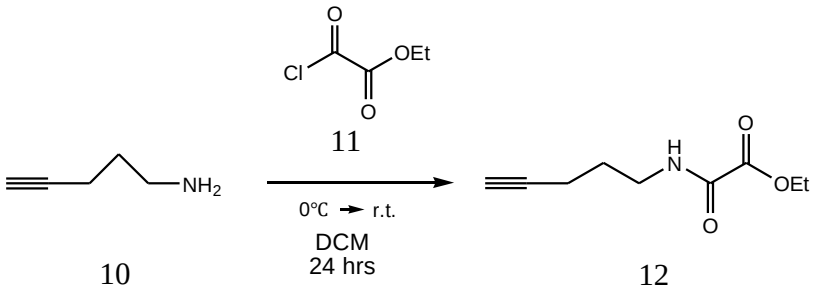


**Scheme 2.8** The synthesis of compound **12**[39]

## 2.3.5 Model Test for the Crude Product of Pentynyl-amine 10

The purification method for 10 does not purify the crude product of di-amine-pyridine 9**.** One possible reason is the compound pentynyl-amine **9** may still exist in aqueous layer and it is hard to extract from water. Therefore during the purification, water should be avoided. The model test for the crude product of pentynyl-amine **10** using no-water purification method can provide very useful reference for the conversion from di-amine-pyridine **9** to di-oxalyl-ethoxy-pyridine **15.**

Since the conditions for hydrazinolysis of pentynyl-phthalimido **7** were optimized, the no-water purification of pentynyl-amine **10** was used as a model. The crude product of pentynyl-amine **10** was filtered first, then the filtrate was collected and dried in vacuum. The resulting mixture contained white solids and oil, which was dissolved in $CH_2Cl_2$ under sonication to better disperse. The mixture was filtered, the filtrate was collected and the solvent was removed under vacuum to afford a pale yellow sticky oil as pentynyl-amine **10.** This product was reacted with ethyl oxalyl chloride to afford ethyl-oxalyl-chloride 13 as an yellow oil with 96% yield.

### 2.3.6 Model Test for Crude Di-amine-pyridine 9

The crude product of the reaction for making pentynyl-amine **10** (Scheme 2.6) was purified by no-water purification and the resulting mixture was used for the latter reaction (Scheme 2.8) to successfully afford pentynyl-ethoxy oxalimide **12**. As a result, the crude product of the reaction to make di-amine-pyridine **9** was purified using the same no-water purification procedures, the NMR spectra did not show clear evidence for di-amine-pyridine **9.** However this resulting mixture was still used to react with ethyl oxalyl chloride to make di-oxalyl-ethoxy-pyridine **15** under the same conditions for preparing pentynyl-ethoxy oxalimide **12** (Scheme 2.8). However neither TLC nor NMR showed any evidence for product.

## 2.3.7 Alternative Route

Since pentynyl-ethoxy oxalimide **12** was prepared with high yield, it is a good choice to test the coupling of dibromopyridine-PEG **5** and pentynyl-ethoxy oxalimide **12** using Sonogashira coupling. (Scheme 2.9)

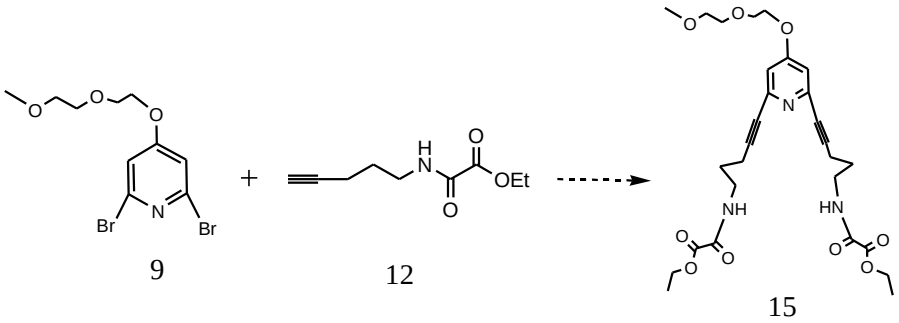


9 12 15

**Scheme 2.9** Sonogashira coupling of compound **5** and **15**

After the reaction of di-phthalimido-pyridine **8** to di-amine-pyridine **9** was found very complicated, an alternative synthetic route was suggested: to use a Boc group to protect the amine first, and then use the Sonogashira reaction to couple to dibromopyridine-PEG **5,** because the Boc protection and deprotection are very reliable.

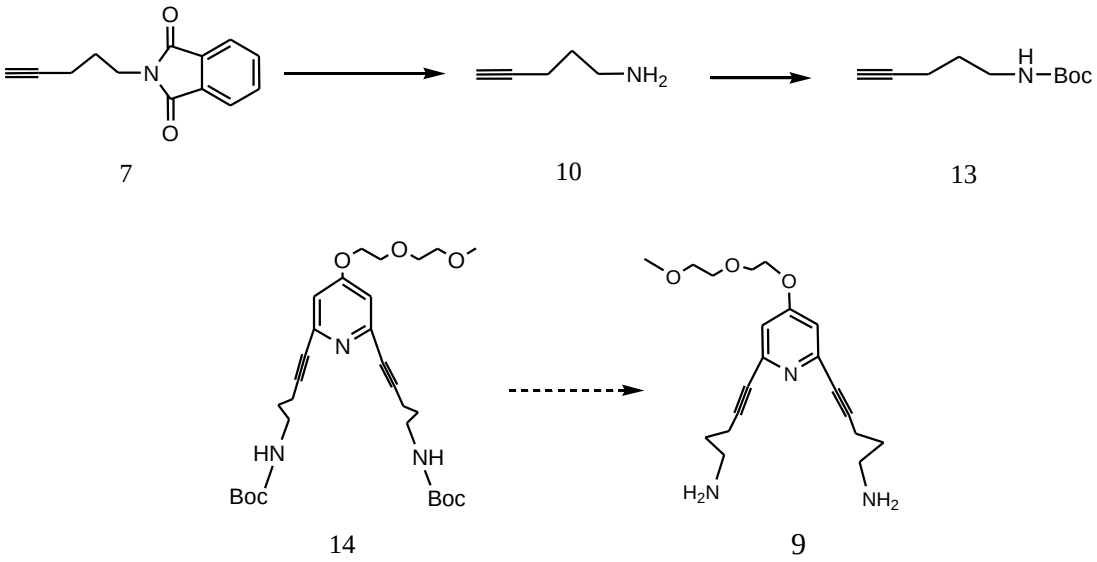


**Scheme 2.10** Alternative route by Boc protection[38]

Pentynyl-amine **10** was dissolved in $CH_2Cl_2$, after 2 hours, the starting material spot on the TLC was still visible. Other literature reports indicated that organic bases such as DMAP and $Et_3N$ are used often for this kind of reaction, usually one equivalent DMAP was introduced to add two Boc groups on an amine. Based on this information, 0.1 equivalent of DMAP was added to the reaction mixture, and after 1 hour the starting material spot on the TLC was much weaker. To make sure the reaction went to completion, this reaction was conducted overnight. However the crude product was not as clean as expected and column chromatography was still needed to purify it.

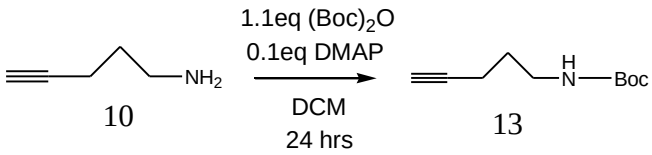


**Scheme 2.11** Boc protection on 1-aminopent-4-yne[38]

The same conditions of di-phthalimido-pyridine **8** preparation were applied to the Sonogashira coupling of pentynyl-amino-boc **13** with dibromopyridine-PEG **5 (**Scheme 2.10**)**. However the result of TLC and silica gel purification indicated that no product was formed.

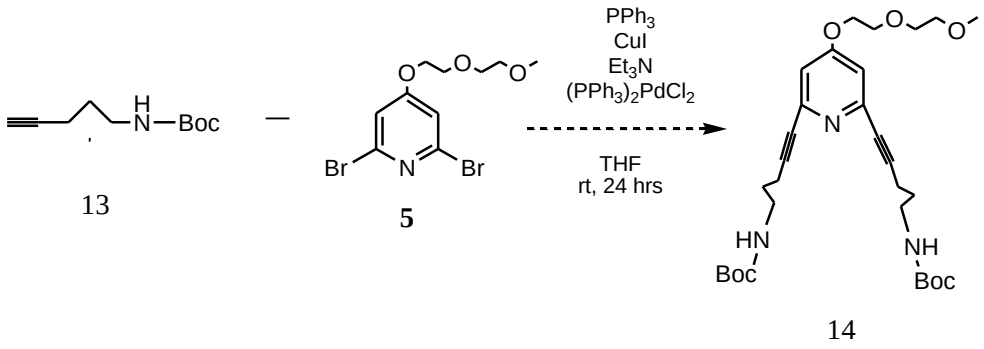


**Scheme 2.12** Sonogashira coupling of **11** and **5**

Safety notes of pentynyl-amino-boc **13**: The MSDS indicates that compound **13** is extremely destructive to the tissue of the mucous membranes and upper respiratory tract. Special caution must be taken.

A new route for clean reaction was also suggested (Scheme 2.13):

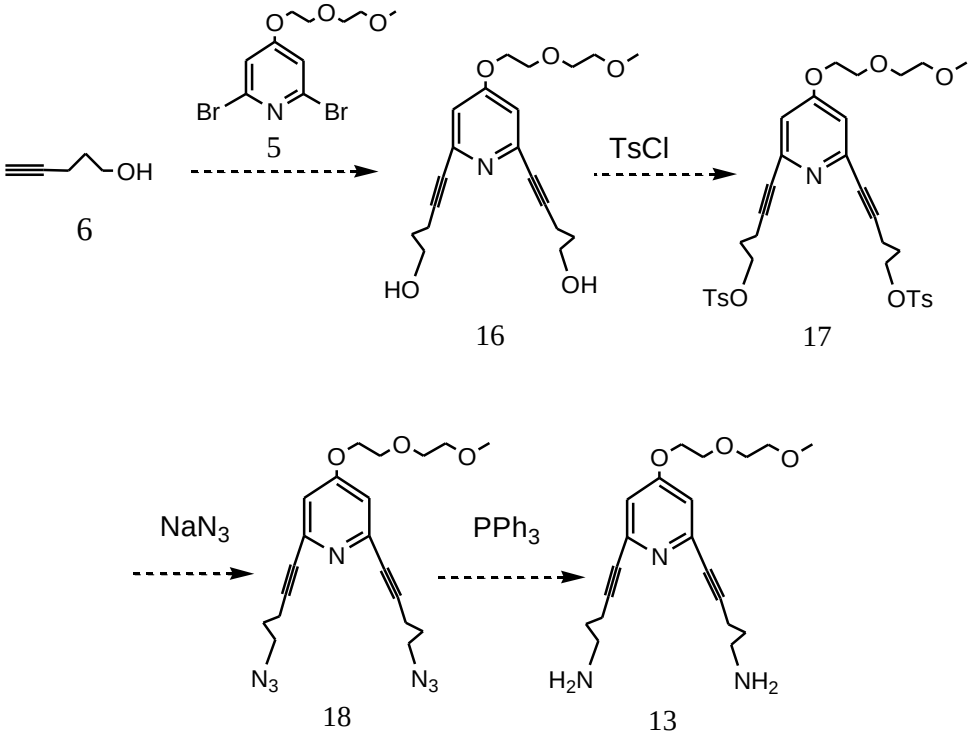


**Scheme 2.13** Future alternative route

Daniel Resch has used a copper-free formula to conduct the Sonogashira reaction below, and the purification was simple so it is very convenient and efficient. (Scheme 2.14)

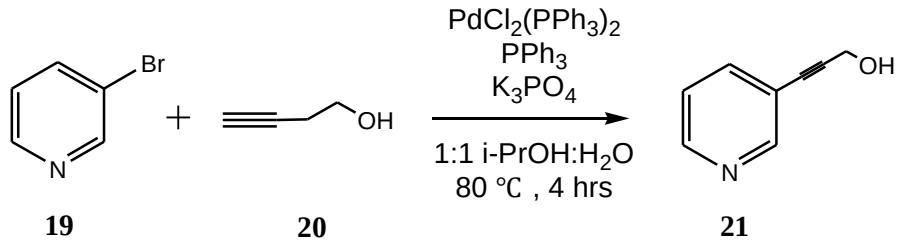


**Scheme 2.14** Copper-free Sonogashira formula

## 2.4 Conclusion

In our project, the geometry of monomer packing is critical to trigger topochemical polymerization. Selecting a suitable host and guest is critical to control the spatial arrangement for topochemical polymerization.

In order to achieve full dehalogenation, it is necessary to develop a new strategy to prevent intermolecular and intramolecular interactions which will cause on-chain iodine crowding, and iodine crowding is the culprit to partial dehalogenation.

For synthesis, the main obstacle lies in the purification of di-amine-pyridine **9**. A new route needs to be proposed to prepare pure di-amine-pyridine **9**, afterwards the reaction with ethyl-oxalyl-chloride **13** may be reliable and clean.

# Chapter 3. Experimental

## 3.1 Conformation Searching Algorithms[28]

The conformer searching algorithms of conformation need to be selected: systematic search or monte-carlo search. Both algorithms consist of the rotation or movement of one or more bonds of certain molecule and energy minimization will be performed afterwards.

## Systematic Search (Grid Search)

It systematically varies each torsion angles to investigate the conformations of the molecule. For example, if one bond can be divided into M different angles and there are N bonds to be examined, the number of calculation is $M^N$.[40] The search of acyclic molecules is to simply rotate each bond by a specified angle (usually 120 degrees). Hence, this method can effectively span the space to find all possible conformations of a small molecule. For cyclic molecules the identical method used is to bend the rings within the molecule successively. Nevertheless the ring conformations are not eventually defined and it may not present a desirable search. Additionally this method is very time consuming for large molecules because the conformation number increases exponentially. As a result, a systematic method should be exclusively applied for small, acyclic molecules. It is still useful big molecules with multiple flexible bonds, but it is used regionally to obtain an energy map of a few significant torsion angles. [27]

## Monte-carlo Search[28]

It uses a method to obtain preferential (minimum energy) conformation by stochastic bond rotations and ring bending within the molecule. For the same computation time, monte-carlo has a better chance of finding low energy conformers than the systematic search. At the beginning

of the calculation it can be imagined that the so-far best conformer is still in a high energy state because it has enough energy so it can be flexible enough to adopt a high energy conformation. This is the advantage of Monte-carlo for that very often the global minimum configuration of a molecule may be quite different from the initial conformation. As the search keeps progressing, the energy decreases, indicating the molecule is more likely to adopt a low energy conformation, also it will have a better chance to obtain a low energy conformer which is closer to other minima in the nearby vicinity.

Monte-carlo was selected after the properties, mechanisms and optimum implementation of the two algorithms above were evaluated.

## 3.2 Method for Molecular Mechanics and Quantum Chemical Calculation[28]

Based on all requirements of molecular mechanics modeling, the function <conformation distribution> was selected to calculate the conformation. The simulation model <molecular mechanics> at <ground state> with <MMFF> force field, used monte-carlo search algorithm, were set. examined 10,000 possible conformers and kept 100 with lowest energy.

HF was selected for quantum chemical calculation with base set 3-21G at ground state in vacuum. These settings balance the calculation quality and time consumption.

## 3.3 Synthesis

## General Information

*Materials*: The diethylene glycol monomethyl ether was purchased from GFS chemicals. The 2,6-Dibromopyridine was purchased from Matrix Scientific. The other chemicals and solvents were purchased from Aldrich, BDH, Alfa Aesar, Fisher Scientific, or Acros Co. and used without purification unless otherwise stated. Flash chromatography was carried out on silica gel 60 (Sorbent Technologies, 230/400 mesh).

*NMR* - $^{1}$H spectra were recorded on Inova-400 NMR (400 MHz) spectrometer and are reported in ppm. Data are reported as: [δ shift]([s= singlet, d=doublet, t=triplet, q=quartet, p=pentet or quintet, m=multiplet, b=broad], [integration], and [J=coupling constant in Hz]). $^{13}$C spectra were recorded on Inova-400 NMR (100 MHz) spectrometer and are reported in ppm.

Purification of CuI[41]: KI (1.82 g) was dissolved in 3.2 mL water. CuI (0.135 g) was dissolved in KI solution. After 1 hour CuI-KI solution was yellow. Charcoal (0.13 g) was added to the solution. The solution color changed from yellow to gray. The solution was stirred for 20 minutes with heating. After stirring, the solution was settled to room temperature and filtered. Cold water 30 mL was added to the orange solution. The orange solution formed a precipitate and it was settled for about 45 minutes, filtered, and dried under vacuum as a white solid

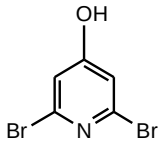


**2**

**2,6-dibromopyridine-4-ol (2)** [29]

2,6-dibromopyridine **1** (2.52 g, 10.7 mmol), 1,2-bis (diphenylphosphino) ethane (97.4 mg, 0.24mmol) and $\{IrCl(cod)\}_2$ (cod=1,5-cyclooctadiene) (142.8 mg, 0.21mmol) were added to a RBF, purged with Ar, and then pinacolborane (5.04 g, 39.4 mmol) was added by syringe. The mixture was stirred under Ar at 130℃ for 4 hours. The resulting mixture was cooled to room temperature, diluted with 40 mL THF, and added into aqueous Oxone solution (61.2g in 306 mL) slowly. The mixture was stirred for 7 min at room temperature becoming a dark green suspension. Followed by quenching with aqueous $NaHSO_3$, the mixture turned brown and released large amount of heat, and the organic layer was formed above the aqueous layer. The mixture was extracted with 20 mL diethyl ether three times. The combined ethereal layers were washed with water and brine, dried over $MgSO_4$, evaporated in vacuo to present a yellow solid. The solid was purified by silica-gel column chromatography (eluent: EtOAc/Hexane 1/5). 1.8 mg, 7.0 mmol (65%) to afford colorless solid. $^1$H NMR (400 MHz, $CDCl_3$): δ 7.06 (s, 1H). $^{13}$C NMR (100 MHz, $CDCl_3$): δ (ppm) 166.7, 140.5, 114.9. [29]

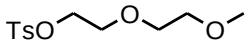


**4**

**2-(2-Methoxy-ethoxy)-ethyl-p-toluene sulfonate (4)** [30]

The solution of NaOH (0.4 g, 10 mmol), and compound **3** (0.84 g, 5 mmol) in 8 mL THF was mixed and cooled down to 0 ℃ by ice bath. TsCl (1.22 g, 6.15 mmol) was dissolved in 2 mL THF first and the solution was added dropwise into the mixture, and then the mixture was stirred for 2 hours at 0 ℃. When the reaction finished, the mixture was poured into cold water (10 mL), extracted with $CH_2Cl_2$ twice, the combined organic layer was washed two times with water and once with brine, dried over $MgSO_4$, filtered and evaporated *in vacuo*. The product was a colorless sticky oil (1.27g, 90%). $^1$H NMR (400 MHz, $CDCl_3$): δ 7.76 (d, 2H, *J*=8.3 Hz), 7.31 (d, 2H, *J*=8.1 Hz), 4.13 (t, 2H, *J*=4.9 Hz), 3.7 (t, 2H, *J*=4.9 Hz), 3.53 (t, 2H, *J*=3.5 Hz), 3.45 (t, 2H, *J*=3.5 Hz), 3.31 (s, 3H), 2.44 (s, 3H). $^{13}$C NMR (100 MHz, $CDCl_3$): δ (ppm) 144.8, 132.9, 129.8, 128.0, 71.8, 70.6, 69.2, 68.7, 59.0, 21.6. [30]

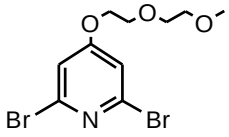


**5**

**2,6-dibromo-4-[2-(2-hydroxyethyloxy)ethyloxy]pyridine (5)**

Dibromopyridine-4-ol **2** (50 mg, 0.198 mmol), tosyl-PEG **4** (61.9 g, 0.218 mmol), and $K_2CO_3$ (0.2 g, 1.45 mmol) were added to an RBF. The mixture was refluxed in acetone for 24 hours. The resulting mixture was filtered through Celite and evaporated in vacuo, affording an orange oil with quantitative yield. $^1$H NMR (400 MHz, $CDCl_3$): δ 6.96 (s, 2H), 4.14 (t, 2H, *J*=4.3 Hz), 3.79 (t, 2H, *J*=4.3 Hz), 3.63 (t, 2H, *J*=4.4 Hz), 3.51 (d, 2H, *J*=4.4 Hz), 3.32 (s, 3H). $^{13}$C NMR

(100 MHz, $CDCl_3$): δ (ppm) 166.9, 141.0, 113.9, 71.9, 70.8, 69.0, 68.4, 50.1.

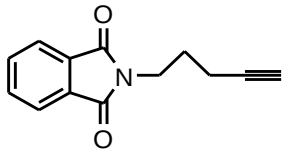

7

**N-(4-Pentynyl)phthalimide (7)**

Pentynyl-ol **6 (**525 mg, 6.25 mmol), $PPh_3$ (1.965 g, 7.49 mmol), phthalimide (1.00 g, 6.80 mmol) and DIAD (4.135 g, 20.45 mmol) were dissolved in 4 vials with 10 mL toluene separately. The solutions of pentynyl-ol **6**, $PPh_3$ and phthalimide were mixed and cooled to 0 ℃, following by the addition of DIAD (1.5890 g, 7.86 mmol), the mixture was kept at 0 ℃. When the addition was finished, the resulting mixture was warmed up to r.t. and stirred for 4 hours. Then 10.5 mL MeOH was added, and the mixture was stirred for another 2 hours. The resulting mixture was evaporated in vacuum to afford the crude product as a yellow sticky oil. The crude product was purified by silica-gel column chromatography (eluent: EtOAc/hexane 1/5) to afford n-(4-pentynyl)phthalimide **7** (1.2 g, 90%) as colorless crystals**.** $^1$H NMR (400 MHz, $CDCl_3$): δ 7.84 (d, 2H, *J*=2.8 Hz), 7.71 (d, 2H, *J*=2.8 Hz), 3.79 (t, 2H, *J*=7.0 Hz), 2.25-2.29 (m, 2H), 1.90-1.97 (m, 3H). $^{13}$C NMR (100 MHz, $CDCl_3$): δ (ppm) 168.5, 134.1, 132.3, 123.4, 83.2, 69.2, 37.3, 27.5, 16.5. [32]

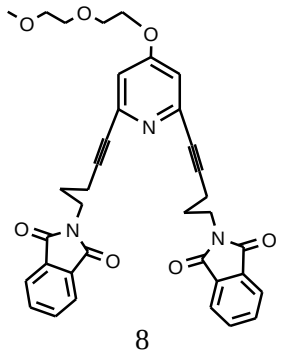

8

**2,6-di-2-(pent-4-ynyl)1H-isoindole-1,3(2H)-dione-4-[2-(2-hydroxyethyloxy) ethyloxy]pyridine (8)**

Sonogashira coupling: dibromopyridine-PEG **5** (386.4 mg, 1.09 mmol), $PPh_3$ (28.5 mg, 2.5 mol%), $(PPh_3)_2PdCl_2$ (152.63 mg, 5 mol%) were added into an RBF and purged with Argon. Pentynyl-phthalimido **7** (878.976 mg, 4.12 mmol) was dissolved in the mixture of 5 mL dry THF and 5 mL $Et_3N$. The solution was added to the RBF by syringe. The mixture was stirred for 15 min under argon and then CuI was added. The whole mixture was stirred for 24 hours. When the reaction was completed, the THF was removed in vacuo. The resulting mixture was diluted with acetone, dried over $MgSO_4$, dried in vacuum to afford the crude product as a yellow solid. The yellow solid was purified with silica-gel column chromatography with eluent: EtOAc/hexane 1/1 to afford 630 mg, 1.02 mmol, 95% yield 8 as dark orange oil. $^1$H NMR (400 MHz, $CDCl_3$): δ 7.77 (t, 4H, *J*=2.5 Hz), 7.65 (t, 4H, *J*=2.5 Hz), 6.70 (s, 2H), 4.11 (t, 2H, *J*=4.3 Hz), 3.79, 3.78 (t, 4H, *J*=6.8Hz), 3.67 (t, 2H, *J*=3.4 Hz ), 3.53 (t, 2H, *J*=4.3 Hz), 3.35 (s, 3H), 2.44 (t, 4H, *J*=7.0 Hz),1.97 (t, 4H, *J*=7.1 Hz). $^{13}$C NMR (100 MHz, D-acetone): δ (ppm) 169.4, 166.2, 146.0, 135.4, 133.7, 124.2, 113.7, 90.1, 82.1, 73.2, 71.8, 70.4, 69.3, 59.4, 38.4, 28.3, 18.0.

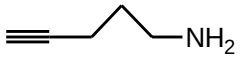

10

**1-aminopent-4-yne (10)** [34]

Pentynyl-phthalimido **7** (800 mg, 3.756 mmol) was dissolved in 10 mL EtOH in an RBF, the solution was purged with Ar. Hydrazine monohydrate (2 equivalents, 375.6 mg, 7.512 mmol) was added to the RBF, and then the mixture was refluxed at 70 ℃ for two hours. The resulting mixture was cooled to room temperature, HCl was added until pH=3, white solid was precipitated. The mixture was filtered and the filtrate was basified to pH=14, following by extraction with $CH_2Cl_2$, dried over $Na_2SO_4$, filtered, and the solvent was removed in vacuo. The product was pale green oil, 221.5mg, 2.67 mmol, 70% yield, no further purification needed. $^1$H NMR (400 MHz, $CDCl_3$): δ 2.81 (t, 2H, *J*=5.5 Hz), 2.21-2.25 (m, 2H), 1.93 (s, 1H), 1.67 (t, 2H, *J*=5.6 Hz). $^{13}$C NMR (100 MHz, $CDCl_3$): δ (ppm) 83.7, 68.6, 40.7, 31.6, 15.7.

13

**Tert-butyl pent-4-ynyl carbamate (11)**[38]

Pentynyl-phthalimido **7** (210.0 mg, 2.53 mmol) was dissolved in $CH_2Cl_2$ at 0℃, $(Boc)_2O$ (551.5 mg, 2.53 mmol) was added dropwise. DMAP (32.6 mg, 0.27 mmol) was added. After the addition was finished, the solution was stirred at r.t. overnight. The resulting mixture was dried in vacuo to afford a yellow oil. The oil was purified with silica-gel column chromatography with

eluent: EtOAc/hexane 1/10 to afford the product as a yellow oil (372.0 mg, 80%). $^{1}$H NMR (400 MHz, $CDCl_3$): δ 4.82 (s, 1H), 3.15 (d, 2H, *J*= 6.3 Hz), 2.15-2.19 (m, 2H), 1.91 (t, 1H, *J*= 2.56 Hz), 1.64 (t, 2H, *J*= 6.9 Hz), 1.33 (s, 9H). $^{13}$C NMR (100 MHz, $CDCl_3$): δ (ppm) 156.0, 83.6, 79.2, 69.0, 39.5 28.7, 28.6, 15.9.

Safety notes: this compound is extremely destructive to the tissue of the mucous membranes and upper respiratory tract. Special caution must be taken.[42]

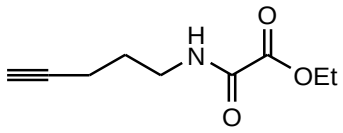


12

**pent-4-ynyl-1-amine-oxalylethoxy (14)**

1-aminopent-4-yne **10 (**137.3 mg, 1.65mmol), $Et_3N$ (1.1 equivalents, 183 mg) were dissolved in an RBF with 10 mL $CH_2Cl_2$. The mixture was purged with Ar and cooled in an ice bath, and then ethyl oxalyl chloride (1 equivalent, 225.8 mg) was dropwise added into the RBF. The mixture was warmed up to room temperature when the addition was finished and stirred for 24 hours. The resulting mixture was purified by silica-gel column chromatography (eluent: EtOAc/hexane 1/1) to afford 3 (302.7, 96% yield) as yellow oil; $^{1}$H NMR (400 MHz, $CDCl_3$), δ(ppm)= 4.32 (q, 2H, *J*= 7.2 Hz), 3.45(q, 2H, *J*= 6.6 Hz), 2.24-2.28 (m, 2H), 2.00 (s, 1H), 1.76 -1.83(m, 2H), 1.36 (t, 3H, *J*= 7.1 Hz), 1.24 (d, 1H, *J*= 6.3 Hz) , $^{13}$C NMR (100 MHz, $CDCl_3$): δ(ppm)= 160.9, 156.9, 83.1, 69.8, 63.4, 39.2, 22.2, 16.3, 14.2.

# Reference


1. Bourzac, Katherine, *MIT Technology Review* **2010.**

2. Kroto, H. W.; Heath, J. R.; O'Brien, S. C.; Curl, R. F.; Smalley. C60: Buckminsterfullerene, *Nature* **1985,***318*, 162–163.

3. Buseck, P. R.; Tsipursky, S. J.; Hettich, R., Fullerenes from the Geological Environment, *Science* **1992**, *257*, 215–217.

4. McQuade, D. T., Pullen, A. E.; Swager, T. M., Conjugated polymer-based chemical sensors, *Chem. Rev*. **2000**, *100*, 2537-2574.

5. Dimitrakopoulos, C. D.; Malenfant, P. R. L., Organic Thin Film Transistors for Large Area Electronics, *Adv. Mater*. **2002**, *14*, 99-117.

6. Nunzi, J. M., Organic photovoltaic materials and devices, *C. R. Phys*. **2002**, *3*, 523-542.

7. Chalifoux, W. A.; Tykwinski, R. R., Synthesis of polyynes to model the sp-carbon allotrope carbyne, *Nature Chemistry* **2010**, *2*, 967-971.

8. Kudryavtsev, Yu. P.; Evsyukov, S. E.; Guseva, M. B.; Babaev, V. G.; Khvostov, V. V., Carbyne-the third allotropic form of carbon, *Russ.Chem.Bull., Int.Ed*. **1993**, *42*, 399-413.

9. Chalifoux, W. A.; Tykwinski, R. R., Synthesis of extended polyynes: Toward carbyne, *C. R. Chimie* **2009**, *12*, 341-358.

10. Wudl, F.; Bitler, S. P., Synthesis and Some Properties of Poly(Diacetylene) (Polyenyne) Oligomers, *J. Am. Chem. Soc*. **1986,** *108*, 4685-4687.

11. Wegner, G. Topochemical Reactions of Monomers with Conjugated Triple Bonds .I. Polymerization of 2.4-Hexadiyn-1.6-Diols Deivatives in Crystalline State, *Chem. Sci*. **1969**, *24*, 824-832.

12. Baughman, R. H., Solid-State Synthesis of Large Polymer Single-Crystals, *J. Polym. Sci., Part B: Polym. Phys*. 1974, 12, 1511-1535.

13. Enkelmann, V., Structural Aspects of the Topochemical Polymerization of Diacetylenes, *Adv. Polym. Sci*., **1984**, *63*, 91-136.

14. Pedersen, C. J., The Discovery of Crown Ethers (Noble Lecture), *Angew. Chem. Int. Ed*. **1988,** *27*, 1021-1027.

15. Cram, D. J.; Cram, J. M., Host-Guest Chemistry: Complexes between organic compounds simulate the substrate selectivity of enzymes, *Science* **1974**, *183*, 803-809.

16. Hirshfeld, F. L.; Schimidt, G. M. J., Topochemical Control of Solid-state Polymerization, *J. Polym. Sci.: Part A* **1964**, *2*, 2181-2190.

17. Kane, L. J.; Nguyen, T,; Xiao J.; Fowler, W. F.; Lauher, W. J., The Host Guest Co-Crystal Approach to Supramolecular Structure, *Mol. Crysr. And Liq. Crysr*. **2001**, *356*, 441-4513.

18. Zhao, Xq; Chang, Yl; Fowler, FW; Lauher, JW; An approach to the design of molecular-solid: The ureylenedicarboxylic acids, *J. Am. Chem. Soc*. **1990**, *112*, 6627-6634.

19. Coe, S.; Kane J. J.; Nguyen, T. L.; Toledo, L. M.; Wininger, E.; Fowler, F. W.; Lauher, J, W., Molecular Symmetry and the Design of Molecular Solids: The Oxalamide Functionality as a Persistent Hydrogen Bonding Unit, *J. Am. Chem. Soc*. **1997**, *119*, 86-93.

20. Politzer, P.; Lane P.; Concha, M. C.; Ma, Y.; Murray, J. S., An overview of halogen bonding, *J. Mol. Model.* **2007**, *13*, 305–311.

21. Di Paolo, T.; Sandorfy, C., On the Hydrogen Bond Breaking Ability of Fluorocarbons Containing Higher Halogens, *Can. J. Chem.* **1974**, *52*, 3612–3622.

22. Sun, A., Lauher, J. W., Goroff, N. S., Preparation of Poly(diiododiacetylene), an Ordered Conjugated Polymer of Carbon and Iodine, *Science* **2006**, *312*, 1030-1034.

23. Luo, L.; Wilhelm, C.; Sun, A.; Grey, C. P.; Lauher, J. W.; Goroff, N. S., Poly(diiododiacetylene): preparation, isolation, and full characterization of a very simple poly(diacetylene), *J. Am. Chem. Soc.* **2008**, *130*, 7702–7709.

24. Luo, L.; Resch, D.; Wilhelm, C.; Young, C. N.; Halada, G. P.; Gambino, R. J.; Grey, C. P.; Goroff, N. S., Room-Temperature Carbonization of Poly(diiododiacetylene) by Reaction with Lewis Bases, *J. Am. Chem. Soc.* **2011**, *133*, 19274-19277.

25. Li, Z.; Fowler, F. W.; Lauher, J. W., Weak Interactions Dominating the Supramolecular Self-Assembly in a Salt: A Designed Single-Crystal-to-Single-Crystal Topochemical Polymerization of a Terminal Aryldiacetylene, *J. Am. Chem. Soc.* **2009**, *131*, 634–643.

26. Yang, J.; Dewal, M. B.; Sobransingh, D.; Smith, M. D.; Xu, Y.; Shimizu, L. S., Examination of the Structural Features That Favor the Columnar Self-Assembly of Bis-urea Macrocycles, *J. Org. Chem.* **2009**, *74*, 102–110.

27. Young, D. C., Computaional Chemistry, *John Wiley & Sons*, Inc. **2001.**

28. (a) Warren J. Hehre, A Guide to Molecular Mechanics and Quantum Chemical Calculations, *Wavefunction, Inc.* **2003**; (b) Tutorial and User's Guide, *Wavefunction, Inc.*, ISBN978-1-890661-38-4.

29. Waki, M; Abe, H.; Inouye, M., Helix formation in synthetic polymers by hydrogen bonding with native saccharides in protic media, *Chem. Eur. J.* **2006**, *12*, 7839-7847.

30. Mihara, T.; Yada, T.; Koide, N., Synthesis and physical properties of poly(phenylene vinylene)s having oligo(ethylene oxide) in the side chain, *Mol. Crysr. and Liq.* **2010**, *411*, 421-437.

31. Yao, Y.; Tian, D.; Li, H., Cooperative Binding of Bifunctionalized and Click-Synthesized Silver Nanoparticles for Colorimetric Co2+ Sensing, *Appl. Mater. Interfaces*, **2010**, *2*, 684–690.

32. (a) Rasberry, R. D.; Smith, M. D.; Shimizu, K. D., Origins of Selectivity in a Colorimetric Charge-Transfer Sensor for Diols, *Org. Lett.* **2008**, *10*, 2889-2892; (b) Malik, G.; Guinchard, X.; Crich, D., Asymmetric Synthesis of Polyhydroxylated N-Alkoxypiperidines by Ring-Closing Double Reductive Amination: Facile Preparation of Isofagomine and Analogues, *Org. Lett.* **2012**, *14*, 596-599; (c)Wu, Y., US patent, Patent number: 7253291, Filing date: Nov 16, 2004, Issue date: Aug 7, **2007,** Application number: 10/989,840.

33. (a) Richardson, C.; Reed, C. A., Synthesis of meso-Extended Tetraarylporphyrins, *J. Org. Chem.* **2007**, *72*, 4750-4755; (b) Hsu, T. J.; Fowler, F. W.; Lauher, J. W., Preparation and Structure of a Tubular Addition Polymer: A True Synthetic Nanotube, *J. Am. Chem. Soc.* **2012**, *134*, 142−145.

34. Wiecek, M.; Kottke, T.; Ligneau, X.; Schunack, W.; Seifert, R.; Stark, H.; Handzlik, J.; Kiec Kononowicz, K., N-Alkenyl and cycloalkyl carbamates as dual acting histamine H-3 and H-4 receptor ligands, *Bioorg. Med. Chem.* **2011**, *19*, 2850–2858.

35. SDBS, Spectral Database for Organic Compounds.

36. Verbeeck, S.; Herrebout, W. A.; Gulevskaya, A. V.; van der Veken, B. J.; Maes, B. U. W., Optimization of Oxidative Alkylamination Reactions through Study of the Reaction Mechanism, *J. Org. Chem.* **2010**, *75*, 5126-5133.

37. Yu, T.; Bai, J.; Guan, Z., Cycloaddition-Promoted Self-Assembly of a Polymer into Well-Defined beta Sheets and Hierarchical Nanofibrils, *Angew. Chem. Int. Ed*. **2009**, *48*, 1097-1101.

38. (a) Denton, T. T.; Zhang, X.; Cashman, J. R., 5-Substituted, 6-Substituted, and Unsubstituted 3-Heteroaromatic Pyridine Analogues of Nicotine as Selective Inhibitors of Cytochrome P-450 2A6, *J. Med. Chem.* **2005**, *48*, 224-239. (b) Augustine, J. K.; Bombrun, A.; Mandal, A. B.; Alagarsamy, P.; Atta, R. N.; Selvam, P., Propylphosphonic Anhydride (T3P®)-Mediated One-Pot Rearrangement of Carboxylic Acids to Carbamates, *Synthesis* **2011**, *9*, 1477–1483.

39. Xu, Y.; McLaughlin, M.; Bolton, E. N.; Reamer, R.A., Practical Synthesis of Functionalized 1,5-Disubstituted 1,2,4-Triazole Derivatives, *J. Org. Chem.* **2010**, *75*, 8666–8669.

40. Conformers, *Accelrys Software Inc*. **2011.** http://accelrys.com/products/datasheets/conformers.pdf

41. Kauffman, G. B.; Fang, L. Y., Purification of Copper(I) Iodide, *Inorg. Synth*. **1983**, *22*, 101–103.

42.MSDS-sigma-aldrich. http://www.sigmaaldrich.com/catalog/product/aldrich/778923?lang=en&region=US

$^1$H NMR spectrum (400 MHz, $CDCl_3$) of compound 5

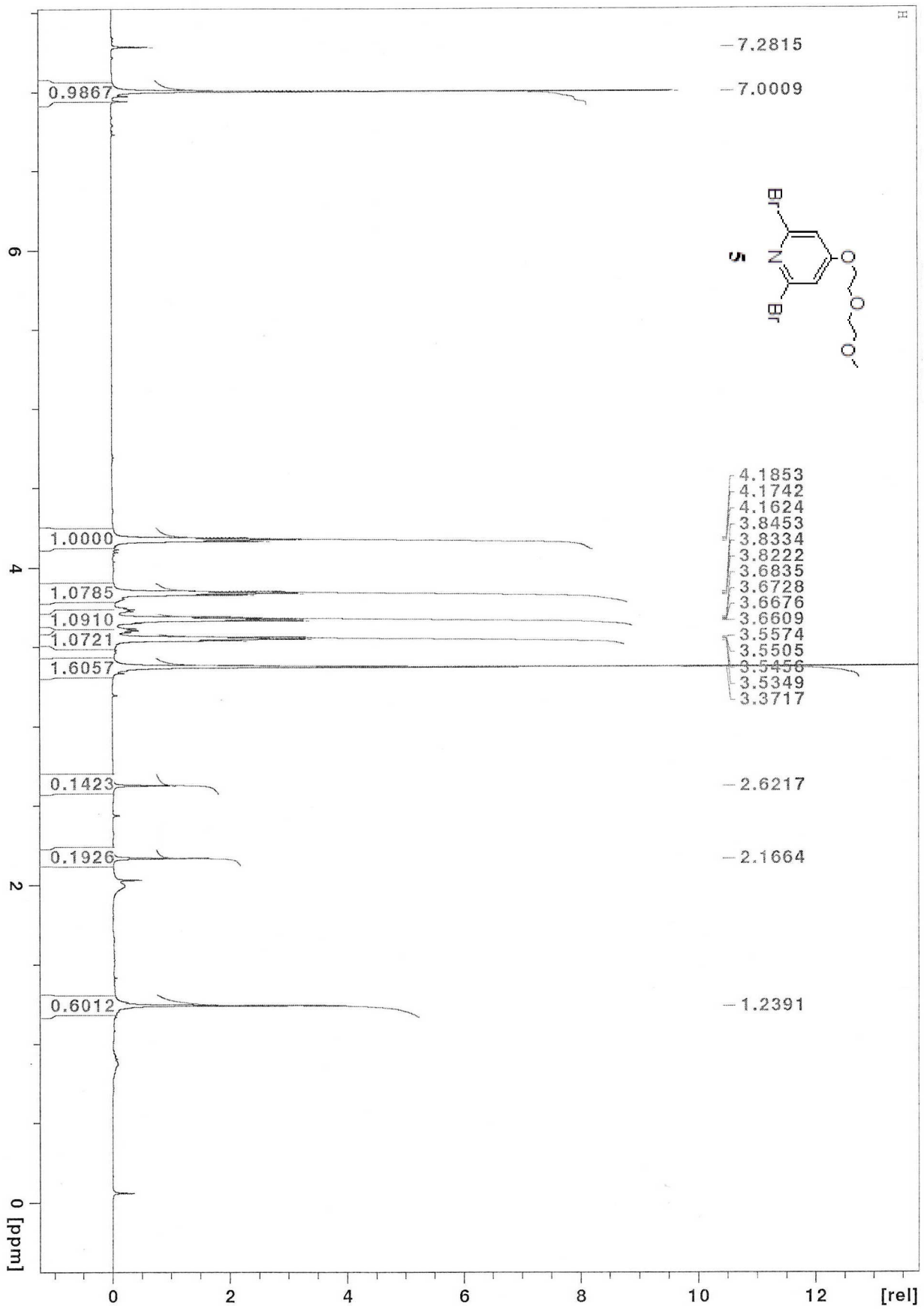

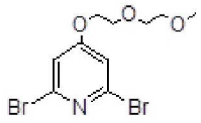


**5**

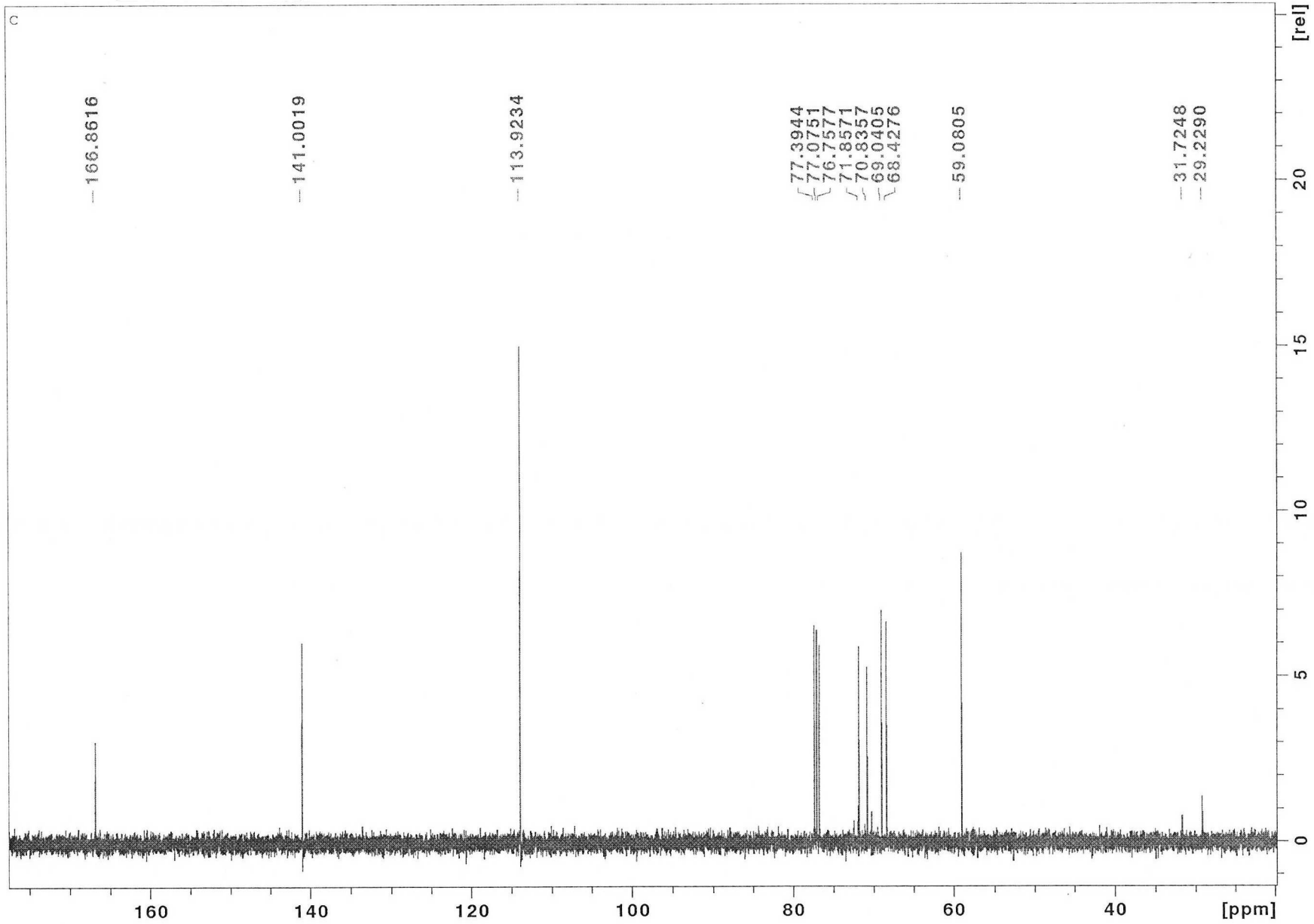


$^{13}C$ NMR spectrum (100 MHz, $CDCl_3$) of compound 5

$^1$H NMR spectrum (400 MHz, $CDCl_3$) of compound 8

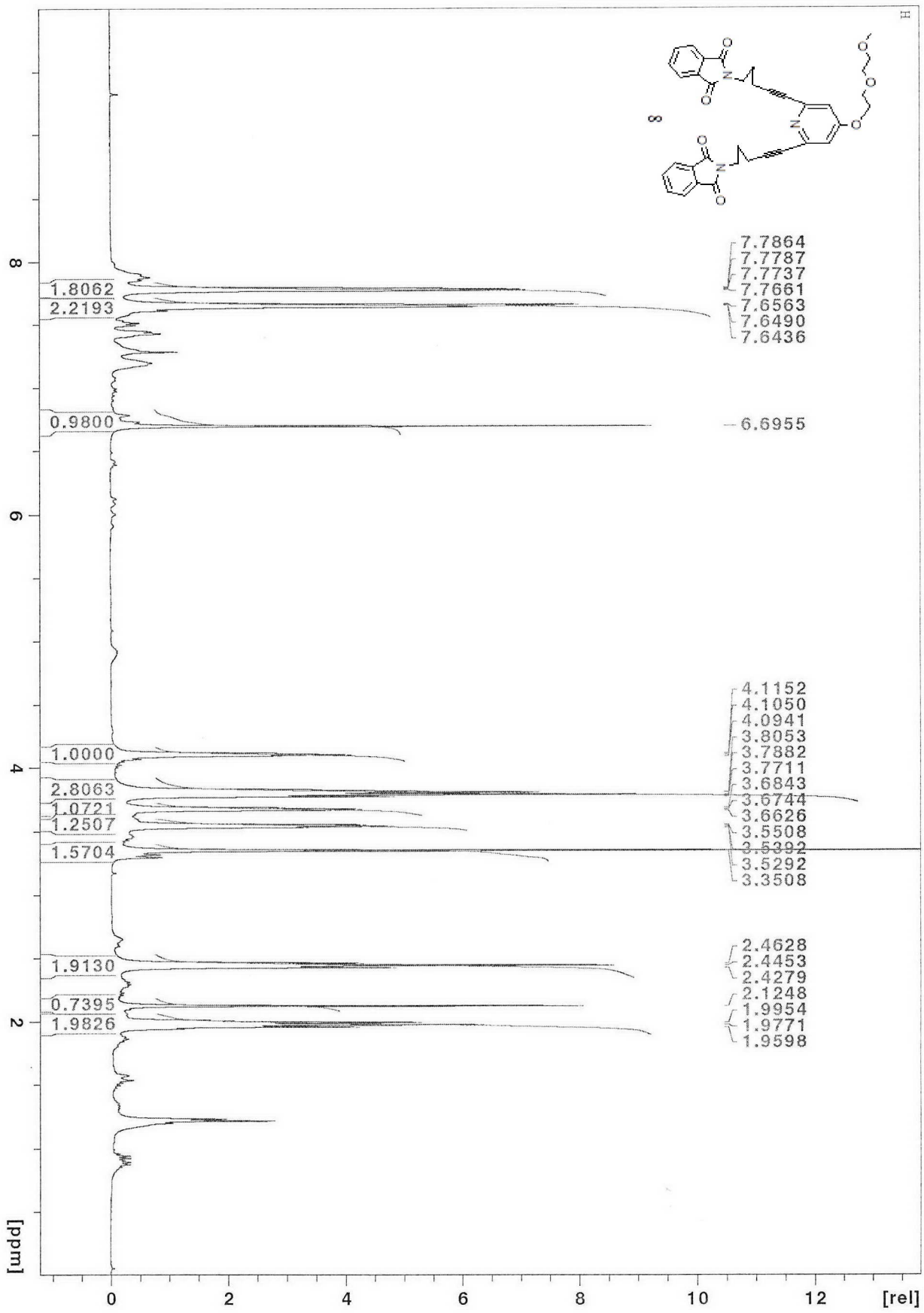

$^{13}$C NMR spectrum (100 MHz, D-acetone) of compound 8

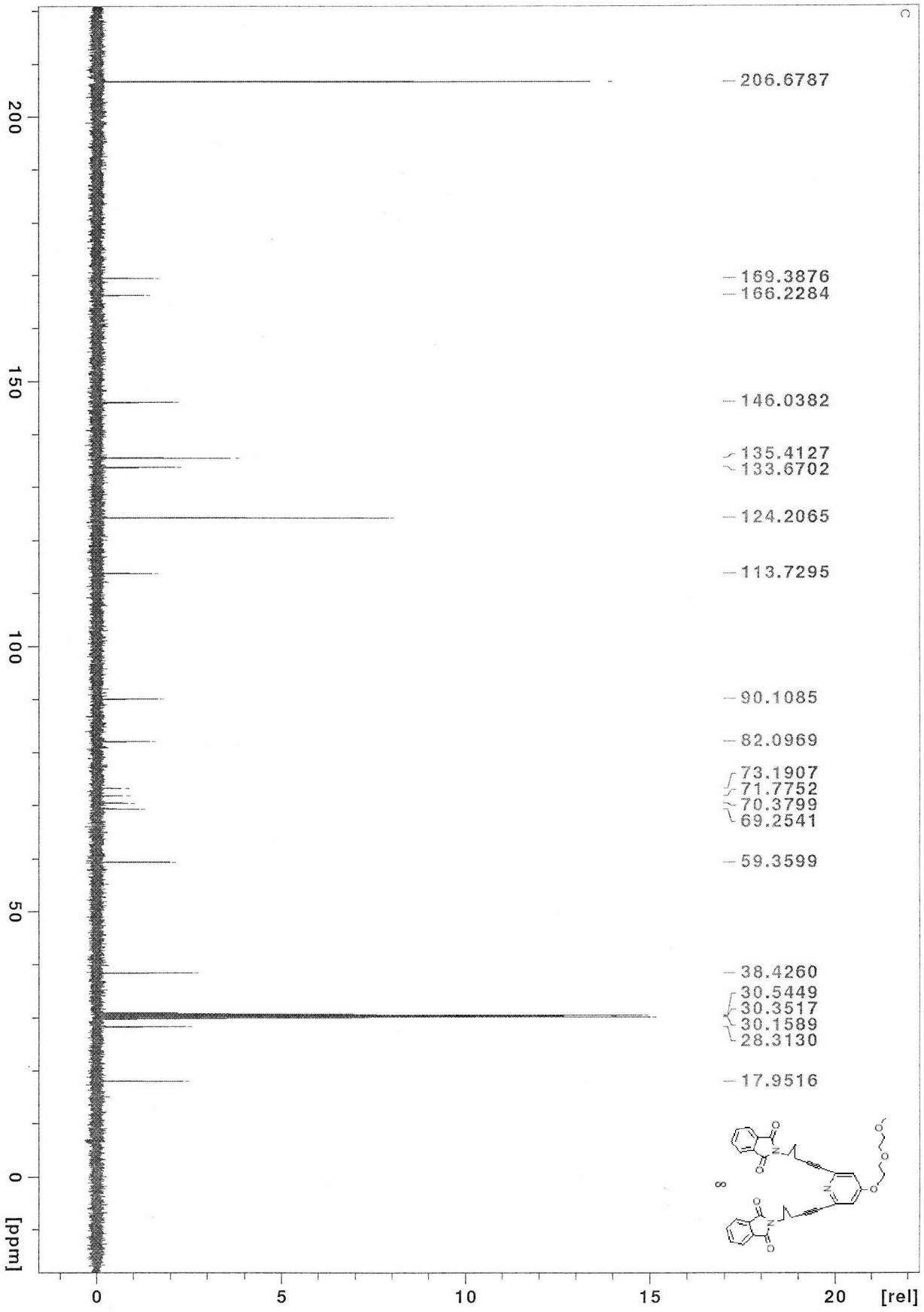

$^1$H NMR spectrum (400 MHz, $CDCl_3$) of compound 12

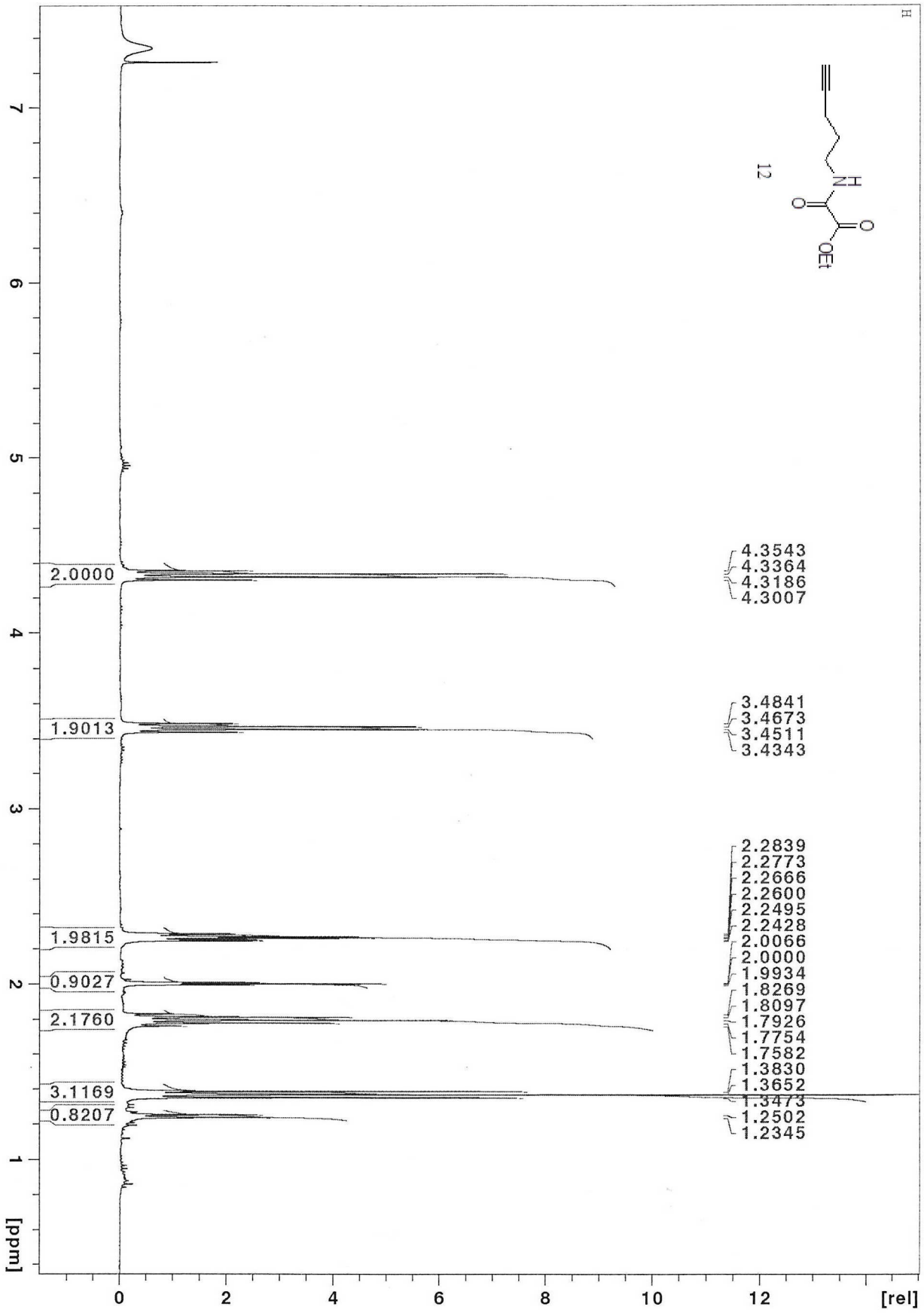

$^{13}$C NMR spectrum (100 MHz, $CDCl_3$) of compound 12